Developmental Biology 453 (2019) 34–47

Contents lists available at ScienceDirect

Developmental Biology

journal homepage: www.elsevier.com/locate/developmentalbiology

Original research article

foxc1 is required for embryonic head vascular smooth muscle differentiation in zebrafish

Thomas R. Whitesell [a,b], Paul W. Chrystal [c,d,e,f], Jae-Ryeon Ryu [a,b], Nicole Munsie [a,b], Ann Grosse [g], Curtis R. French [d,e,f,1], Matthew L. Workentine [h], Rui Li [g], Lihua Julie Zhu [g,i], Andrew Waskiewicz [d,e,f], Ordan J. Lehmann [c], Nathan D. Lawson [g], Sarah J. Childs [a,b,*]

[a] Alberta Children's Hospital Research Institute, University of Calgary, Canada
[b] Department of Biochemistry and Molecular Biology, University of Calgary, 3330 Hospital Drive NW, Calgary, Alberta, Canada, T2N 4N1
[c] Departments of Ophthalmology, and Medical Genetics, University of Alberta, Edmonton, Alberta, Canada
[d] Department of Biological Sciences, CW405, Biological Sciences Bldg., 11455, Saskatchewan Dr., University of Alberta, Edmonton, AB, T6G 2E9, Canada
[e] Women & Children's Health Research Institute, ECHA 4-081, 11405 87, Ave NW, University of Alberta, Edmonton, AB, T6G 1C9, Canada
[f] Neurosciences and Mental Health Institute, 4-120 Katz Group Centre, University of Alberta, Edmonton, AB, T6G 2E1, Canada
[g] Department of Molecular, Cell, and Cancer Biology, University of Massachusetts Medical School, 364 Plantation Street, Worcester, MA, USA, 01605
[h] Faculty of Veterinary Medicine, University of Calgary, 3330 Hospital Drive NW, Calgary, Alberta, Canada, T2N 4N1
[i] Program in Bioinformatics and Integrative Biology, Program in Molecular Medicine, University of Massachusetts Medical School, Worcester, MA, USA, 01605

ARTICLE INFO

Keywords:
foxc1b
acta2
Vascular smooth muscle cell
Zebrafish
CRISPR
RNA-Seq transcriptome

ABSTRACT:

Vascular smooth muscle of the head derives from neural crest, but developmental mechanisms and early transcriptional drivers of the vSMC lineage are not well characterized. We find that in early development, the transcription factor *foxc1b* is expressed in mesenchymal cells that associate with the vascular endothelium. Using timelapse imaging, we observe that *foxc1b* expressing mesenchymal cells differentiate into *acta2* expressing vascular mural cells. We show that in zebrafish, while *foxc1b* is co-expressed in *acta2* positive smooth muscle cells that associate with large diameter vessels, it is not co-expressed in capillaries where *pdgfrβ* positive pericytes are located. In addition to being an early marker of the lineage, *foxc1* is essential for vSMC differentiation; we find that *foxc1* loss of function mutants have defective vSMC differentiation and that early genetic ablation of *foxc1b* or *acta2* expressing populations blocks vSMC differentiation. Furthermore, *foxc1* is expressed upstream of *acta2* and is required for *acta2* expression in vSMCs. Using RNA-Seq we determine an enriched intersectional gene expression profile using dual expression of *foxc1b* and *acta2* to identify novel vSMC markers. Taken together, our data suggests that *foxc1* is a marker of vSMCs and plays a critical functional role in promoting their differentiation.

1. Introduction

Defects in vascular mural cells lead to vascular dysfunction including cerebral small vessel disease and stroke (French et al., 2014; Joutel et al., 1996; Baron-Menguy et al., 2017; Craggs et al., 2014). For example, loss of vSMCs results in thoracic aneurysm and dissections (TAAD) (Guo et al., 2009) and increased vessel size due to poor smooth muscle contraction (Abrams et al., 2016), while loss of pericytes can lead to increased brain permeability, aneurysm, and hemorrhage (Lindahl et al., 1997; Moura et al., 2017). Knowledge of the transcriptional pathways leading to vSMC differentiation is poor, and hampers efforts to regenerate these cells after disease or injury.

Vascular smooth muscle cells (vSMCs) and pericytes (collectively known as vascular mural cells) encircle and stabilize the underlying endothelium, deposit extracellular matrix proteins, and provide contractility to blood vessels (Lindahl et al., 1997; Armulik et al., 2011; Stratman et al., 2009, 2017; Santoro et al., 2009; Carmeliet and Jain, 2011; Whitesell et al., 2014). vSMCs typically form a multilayer, continuous sheath on large caliber blood vessels subject to higher blood pressure. Found outside the basement membrane in mammals, vSMCs provide physical support and actively contract (Stratman et al., 2017; Santoro et al., 2009; Whitesell et al., 2014; Olson and Soriano, 2011;

* Corresponding author. Department of Biochemistry and Molecular Biology, University of Calgary, 3330 Hospital Drive NW, Calgary, Alberta, T2N 4N1, Canada.
E-mail address: schilds@ucalgary.ca (S.J. Childs).
[1] Current address: Discipline of Genetics, Memorial University, St. John's, Newfoundland and Labrador, Canada.

https://doi.org/10.1016/j.ydbio.2019.06.005
Received 8 April 2019; Received in revised form 29 May 2019; Accepted 9 June 2019
Available online 11 June 2019

Etchevers et al., 2001). On the other hand, pericytes are punctate, non-continuous cells with individual processes that wrap around smaller diameter blood vessels creating peg and socket connections with the endothelium. Pericytes are essential in regulating vascular permeability in the blood-brain barrier, and are more prevalent at branching points of blood vessels, turbulent areas of blood flow, or bends in complex blood vessels (Armulik et al., 2011; Stratman et al., 2017; Whitesell et al., 2014; Olson and Soriano, 2011; Etchevers et al., 2001; Bergers and Song, 2005; Berthiaume et al., 2018; Winkler et al., 2010; Trost et al., 2016; Van Dijk et al., 2015; Craggs et al., 2015; He et al., 2016; Birbrair et al., 2017; Dias Moura Prazeres et al., 2017; Hellström et al., 1999).

Smooth muscle actin (*acta2/αsma*) and transgelin (*tagln/sm22α-b*) are the most widely used vSMC markers in zebrafish (Santoro et al., 2009; Whitesell et al., 2014; Seiler et al., 2010; Georgijevic et al., 2007). Zebrafish pericytes, on the other hand, are typically labelled with platelet-derived growth factor receptor-beta (*pdgfrβ*) (Armulik et al., 2011; Stratman et al., 2017; He et al., 2016; Ando et al., 2016), *notch3* (Wang et al., 2014), *abcc9* (Armulik et al., 2011; He et al., 2016; Vanlandewijck et al., 2018), or *desmin* (Armulik et al., 2011; Trost et al., 2016; Georgijevic et al., 2007). In zebrafish, expression from transgenic *acta2* and *tagln* is first detectable around 3 days post fertilization (dpf), with robust vSMC expression by 4 dpf (Santoro et al., 2009; Whitesell et al., 2014; Seiler et al., 2010; Georgijevic et al., 2007; Gays et al., 2017; Majesky, 2007); however, vascular mural cells are already present prior to these markers being expressed. We previously observed mural cells with a mesenchymal phenotype associated with the endothelium as early as 48 h post fertilization (hpf) using transmission electron microscopy, correlating with timelines of vascular stabilization (Liu et al., 2007; Lamont et al., 2010). Here we seek to understand the earliest stages of vSMC development by identifying an early expressed marker.

Since many vSMCs of the head are neural crest-derived, we searched for transgenic markers that are first expressed in neural crest and label vSMCs later in development. One potential marker in zebrafish is the forkhead box domain transcription factor *foxc1b*. Data in mouse and human are supportive of a role for *Foxc1* in mural cells. *Foxc1* is expressed in mouse brain pericytes and vSMCs and is co-expressed with both *Pdgfrβ* and *Acta2* at E14.5 [36–39]. It is also expressed in neural crest (Siegenthaler et al., 2013; Seo et al, 2012, 2017; Kume et al., 1998) and in the endothelium (Kume et al, 1998, 2001; Koo and Kume, 2013). Loss of *Foxc1* in mouse leads to severe defects in head mesenchyme, branchial arch and anterior somite development (Kume et al, 1998, 2001), as well as disrupted pericyte contacts on the endothelium and cerebral hemorrhage (French et al., 2014; Siegenthaler et al., 2013; Prasitsak et al., 2015; Mishra et al., 2016; Kume et al., 1998), but no defects in *Acta2* expression (Kume et al., 2001). Mouse *Foxc1* plays an important role in vascular development (Prasitsak et al., 2015; Mishra et al., 2016; Seo et al., 2012; Kume et al., 2001; Koo and Kume, 2013; Skarie and Link, 2009; Veldman and Lin, 2012; Hayashi and Kume, 2008a, 2008b; Yamagishi et al., 2003); cardiac outflow tract development (Kodo et al., 2017; Seo and Kume, 2006); somitogenesis (Kume et al., 2001; Topczewska et al., 2001); neural crest development (Seo et al., 2012; Seo and Kume, 2006); and hematopoiesis (Omatsu et al., 2014). In humans, *FOXC1* is associated with anterior segment dysgenesis in the eye, cerebral small vessel disease, glaucoma, and Axenfeld-Rieger syndrome (French et al., 2014; Seo et al., 2017; Kume et al., 2001; Mears et al., 1998; Nishimura et al., 1998; Avasarala et al., 2018; Souzeau et al., 2017).

In zebrafish, there are two *foxc1* paralogs, *foxc1a* and *foxc1b* (Skarie and Link, 2009; Topczewska et al., 2001; Chen et al., 2017). *foxc1b* is first expressed during the involution of mesendoderm in early gastrulation, and by 33 hpf, it is expressed in the pharyngeal arch mesenchyme (Topczewska et al., 2001). Morpholino knockdown of *foxc1a/b* in zebrafish shows a reduction in *acta2* positive vSMCs in the ventral aorta and aortic arch arteries (French et al., 2014), suggesting it promotes mural cell development; however, this role is not well defined. *foxc1* expression is also reported in the endothelium of mouse and in the trunk endothelium of zebrafish where it plays an early cell-autonomous role in endothelial differentiation (Siegenthaler et al., 2013; Prasitsak et al., 2015; Mishra et al., 2016; Kume et al., 1998; Skarie and Link, 2009; Topczewska et al., 2001; Winkler et al., 2018).

Here, we probe the role of *foxc1* in head vSMC development; we show that *foxc1b* labels smooth muscle precursors and differentiated vSMCs, not pericytes in fish. We identify and visualize a key window for attachment of *foxc1b:EGFP* positive vSMCs to the endothelium. Using genetic mutants and genetic ablation we then show that vSMC differentiation is impaired in compound *foxc1a/foxc1b* mutants and after ablation of *foxc1b* expressing cells, suggesting that *foxc1* is essential for vSMC differentiation. Finally, the transcriptome of dual *foxc1b* + *acta2* expressing cells uncovers a set of enriched genes specific to the embryonic head vSMC population during early differentiation.

2. Results

2.1. foxc1b is expressed in mesenchymal cells that attach to the endothelium

The earliest stages of migration and attachment of mural cells to the endothelial wall have not been observed in real time in any species. We hypothesized that the early expression of *foxc1b* in neural crest would allow us to visualize this process. *foxc1b* expression can be visualized using the transgenic line, *Tg(-5.0kbfoxc1b:EGFP)^{mw44}* (Miesfeld and Link, 2014). At 2 dpf, when we have previously seen vascular mural cells present near the endothelium of the dorsal aorta using transmission electron microscopy (Liu et al., 2007; Lamont et al., 2010), *foxc1b:EGFP* expressing cells are near the endothelium and have a mesenchymal morphology (Fig. 1A). By 3 dpf, *foxc1b:EGFP* positive cells associate closely with the endothelium (Fig. 1B, arrowheads). At 4 dpf, differentiated mural cells in this region continue to express *foxc1b:EGFP* (Fig. 1C), suggesting that *foxc1b* is expressed both in precursors and differentiated vSMCs.

To trace when *foxc1b:EGFP* expressing cells transform from a mesenchymal to a smooth muscle morphology we used time-lapse confocal microscopy. *foxc1b:EGFP* positive cells begin as mesenchymal clusters adjacent to *kdrl:mCherry* positive endothelium (Fig. 2). Distinct *foxc1b:EGFP* positive vascular mural cells are seen on the endothelium by 58 hpf (Fig. 2A and B, Movie 1). After taking on a smooth muscle cell morphology, vessel associated *foxc1b:EGFP* positive cells then express *acta2*. This transition from *foxc1b:EGFP+; acta2:mCherry-* to *foxc1b:EGFP+; acta2:mCherry+* occurs around 66 hpf (Fig. 2C–E, Movie 2). Thus, our data suggest that *foxc1b* expressing mesenchymal cells closely associate with the endothelium, morphologically differentiate into vSMCs expressing *acta2*, and that *foxc1b* expression precedes *acta2* expression.

2.2. foxc1b expressing mural cells are smooth muscle and not pericyte precursors

The bulbus arteriosus and adjacent ventral aorta are the first sites in the zebrafish embryo to develop vSMC coverage (Whitesell et al., 2014). *foxc1b* is expressed in neural crest and is necessary for *acta2* expression in morpholino knockdown studies (French et al., 2014), but is it also necessary for pericyte development? There has been no characterization of *foxc1b:EGFP* expression in vascular mural cells, therefore we first verified the transgenic line faithfully mimics endogenous *foxc1b* expression. Comparing *foxc1b* mRNA expression at 2 and 4 dpf, patterns between the endogenous gene and transgenic line are very similar (Figs. S1A, C, E, G, I, and L). Specifically, *foxc1b* mRNA is expressed in the aortic arches, jaw, ceratohyal cartilage (Filipek-Górniok et al., 2015; Knight, 2003; Schilling et al., 1996; Xu et al., 2018) and in the periocular mesenchyme in the ventral head. Furthermore, *foxc1b* mRNA expression overlaps with *foxc1b:EGFP* transgenic expression in the ventral aorta, aortic arch arteries, and ceratohyal at 2 and 4 dpf (Figs. S1B, D, F, H, J, and M). As GFP has perdurance, we also compared expression of *egfp*

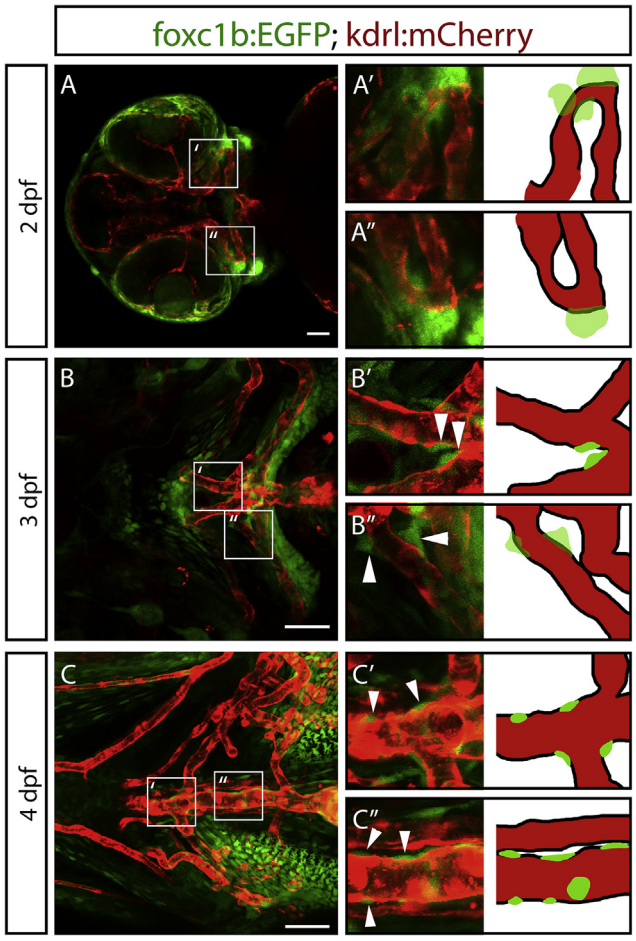

Fig. 1. *foxc1b:EGFP* expressing mesenchymal cells attach to vessels and take on a vSMC morphology. A) Images of the ventral head in 2 dpf zebrafish embryos show *foxc1b:EGFP* positive mesenchymal cells near the endothelium (*kdrl:mCherry*; n = 19 embryos). B) At 3 dpf, *foxc1b:EGFP* positive cells associate with the endothelium (n = 14 embryos). Arrowheads indicate mural cells associated with the endothelium. C) At 4 dpf, *foxc1b:EGFP* positive cells flatten and tightly associate with the endothelium (n = 11 embryos). Scale bars represent 50 μm.

mRNA in the transgenic line to EGFP protein (Fig. S1K and N). Strong co-expression suggests *EGFP* is actively expressed at both the mRNA and protein levels from the *foxc1b* promoter at 4 dpf when vSMCs differentiate.

We tested whether *foxc1b:EGFP* is co-expressed with either pericyte or vSMC markers at 4 dpf when robust expression of vSMC and pericyte markers is present in zebrafish embryos (Santoro et al., 2009; Whitesell et al., 2014; Seiler et al., 2010; Wang et al., 2014). As detectable using zebrafish transgenic markers, *acta2* and *pdgfrβ* transgenic lines show little to no co-expression in the ventral head (Fig. S3). This allows us to distinguish vSMCs and pericytes, respectively. *foxc1b:EGFP* positive cells are located adjacent to, and in close contact with, the endothelium of the ventral aorta (Fig. 3A, arrowheads) with a similar morphology to vSMCs that express *acta2:EGFP* (Fig. 3B). We find that *foxc1b:EGFP* and *acta2:mCherry* are co-expressed in vSMCs (Fig. 3C, arrows). Endogenous *foxc1b* mRNA is also expressed in cells adjacent to the endothelium (as marked by *kdrl*) and is co-expressed with *acta2* in vSMCs (Fig. S2). *foxc1b:EGFP* is not expressed in pericytes at 4 dpf as shown by analysis of double transgenic *foxc1b:EGFP* and *pdgfrβ:Gal4FF; UAS:NTR-mCherry* (hereafter *pdgfrβ:mCherry*; Fig. S3).

Co-expression patterns of *foxc1b* in head vSMCs persist through 9 and 12 dpf (Fig. S4). Furthermore, *foxc1b:EGFP* and *acta2:mCherry* are also co-expressed in vSMCs on the dorsal aorta of the trunk at 4 dpf. Although *foxc1b* mRNA expression has been noted in 48 hpf trunk embryonic endothelium (Chen et al., 2017), we note no endothelial transgene expression in the trunk at the later 4 dpf stage using the *foxc1b:EGFP* transgenic line (Fig. S5).

Co-expression of *acta2* and *foxc1b* is not universal, and cells expressing either *foxc1b:EGFP* or *acta2:mCherry* are occasionally observed (Fig. S4). The percentage of vSMCs expressing *foxc1b* only, *acta2* only, or both *foxc1b* + acta2 is constant between 3 and 4 dpf. At 4 dpf, a total of 83.8% of vSMCs express *foxc1b,* and 72.1% express *acta2.* Conversely, 25.4% of vSMCs express only *foxc1b,* while 16.2% of vSMCs express only *acta2* (Fig. S6). This suggests the majority of vSMCs are double positive for both *foxc1b* and *acta2* expression.

2.3. *foxc1b is expressed in smooth muscle cells in the adult zebrafish brain*

To understand if *foxc1b* is a marker only for developing vSMCs, or is expressed in the adult, we next tested whether *foxc1b* is expressed in vSMCs in the adult brain. We find that embryonic co-expression patterns of *foxc1b*, *acta2* and *pdgfrβ* are similar to those in the adult. In the adult brain, vessel associated *foxc1b:EGFP* expressing cells are associated with large arterioles, but not smaller capillaries (Fig. 4A), similar to the distribution of *acta2:EGFP* expressing cells on arterioles and not on capillaries (Fig. 4B). *foxc1b:EGFP* is almost always co-expressed with *acta2:mCherry*; however, there are regions of *acta2:mCherry* expression that lack co-expression of *foxc1b:EGFP* (Fig. 4C), particularly on the largest diameter vessels. In these experiments, we did not detect *foxc1b:EGFP* on the same vessels that express *pdgfrβ:mCherry* in the adult brain, and *foxc1b:EGFP* is not expressed in endothelial cells. Thus, in both the embryo and the adult brain, *foxc1b* is expressed in vSMCs.

2.4. *foxc1b expression scales with vessel diameter and location in both embryos and adults*

As an animal grows, its vessels enlarge to increase the supply of blood to growing tissues. Little is known about how mural cell subtypes change over development with regard to diameter, anatomical location or developmental timing. The identification of early vSMC markers allows us to test whether mural cell subtypes associate with vessels of consistent sizes and whether this is consistent among vessel beds. To test this, we measured the diameter of the *kdrl* positive endothelial lining and correlated this with mural cell marker expression (*pdgfrβ, foxc1b,* or *acta2*) in the ventral head (ventral aorta, opercular artery, hypobranchial artery, aortic arch arteries, and lateral dorsal aorta), embryonic brain (central arteries, primordial hindbrain channel, basilar artery, and the internal carotid artery), and adult brain. In the embryonic ventral head at 4 dpf, we find that naked vessels (labelled by endothelial *kdrl*, but unlabelled with mural cell markers) have a mean diameter of 9.7 ± 2.0 μm (Fig. 5A and B). The vessels covered with pericytes (*pdgfrβ*) have a mean vessel diameter of 10.3 ± 2.1 μm, and are not significantly different in size from naked vessels. *foxc1b* covered vessels have a mean diameter of 14.6 ± 4.4 μm, and *acta2* covered vessels have a mean of 14.1 ± 4.5 μm, while *foxc1b* + *acta2* covered vessels are the largest, with a mean diameter of 20.5 ± 6.8 μm. Thus, as one might expect, vSMC covered vessels are significantly larger than naked or pericyte covered capillaries. The cluster of larger diameter *foxc1b* + *acta2* double positive vessel data reflects the strong co-expression of *acta2* and *foxc1b* in the ventral aorta, which is the largest vessel at 4 dpf (Fig. 5).

The embryonic brain develops smooth muscle coverage later than vessels in the ventral head, most likely as the blood flow in the brain is lower in early development, and blood flow is important for recruitment of mural cells (Chen et al., 2017). Interestingly, we found no expression of *foxc1b* around vessels in the 4 dpf zebrafish brain. The mean vessel diameter for naked brain vessels at 4 dpf is 7.5 ± 2.0 μm while it is 8.1 ± 2.2 μm for *pdgfrβ* covered vessels (Fig. 5C and D). Both naked *kdrl* and *pdgfrβ* covered vessel diameters are significantly smaller than *acta2* covered vessels (14.4 ± 2.5 μm).

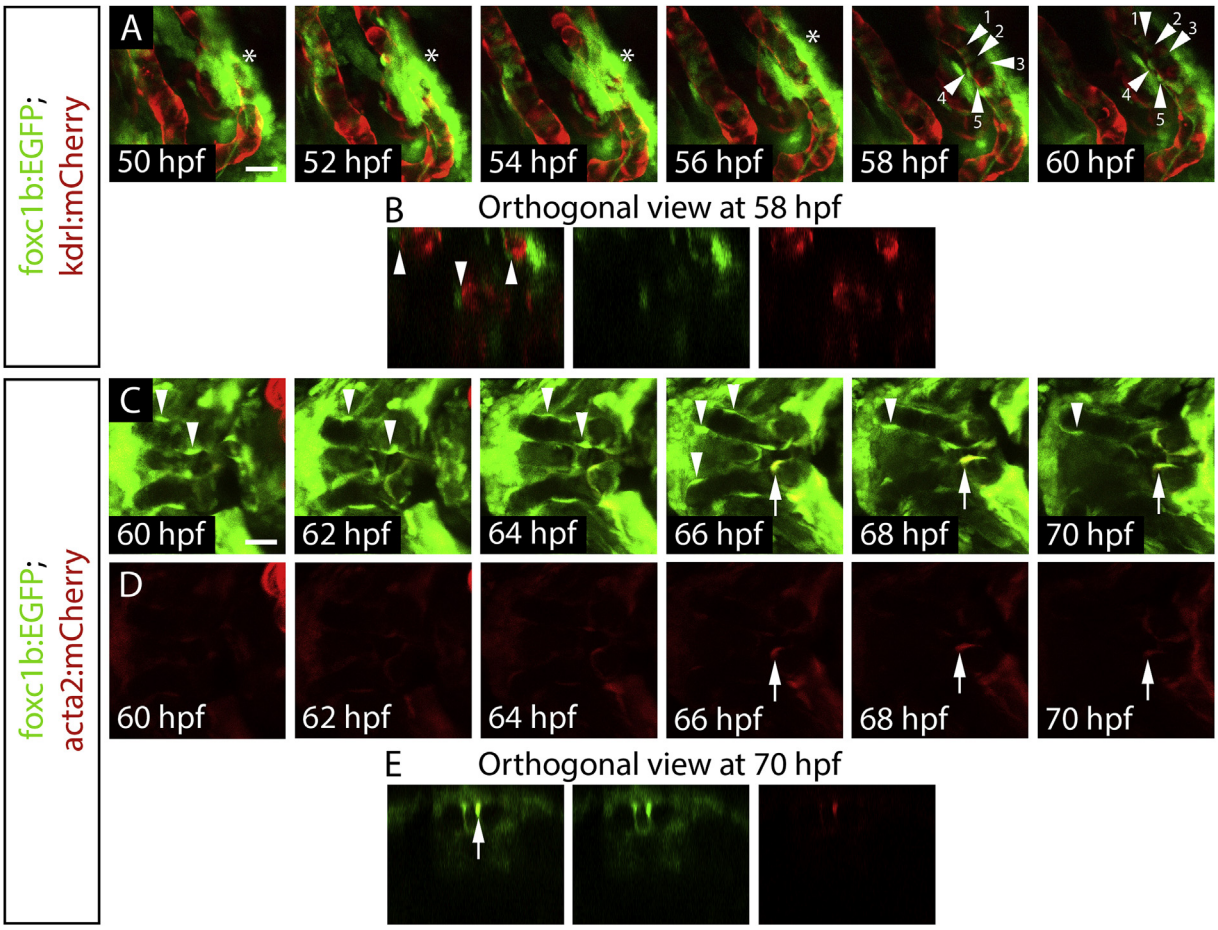

Fig. 2. Timelapse of *foxc1b* expressing mesenchymal cells attaching to the endothelium followed by upregulation of *acta2*. A) Ventral views of aortic arch arteries of a *foxc1b:EGFP; kdrl:mCherry* embryo using confocal time-lapse imaging starting at 50 hpf. Mesenchymal cells are indicated by the asterisk, while vascular mural cells are indicated by arrowheads, starting by 56–58 hpf. B) Orthogonal views at 58 hpf depict the *foxc1b:EGFP* cells wrapping around, but not co-expressing an endothelial marker. C) Time-lapse of the early ventral aorta of a *foxc1b:EGFP; acta2:mCherry* embryo from 60 to 70 hpf. *foxc1b:EGFP* positive smooth muscle cells are associated with the endothelium (arrowheads) but do not co-express *acta2:mCherry* until approximately 66 hpf (arrow). D) Single channel images of *acta2:mCherry*. E) Orthogonal views at 70 hpf show *acta2:mCherry* co-expressed within a *foxc1b:EGFP* positive cell. Scale bars represent 20 μm.

In the adult brain, the mean vessel diameter for naked capillaries is 5.6 ± 2.0 μm and for *pdgfrβ* covered capillaries it is significantly larger at 9.4 ± 5.2 μm. The mean vessel diameter of vessels expressing any combination of *foxc1b* or *acta2* markers is not significantly different. *foxc1b* covered vessels have a mean diameter of 17.2 ± 11.2 μm, *acta2* covered vessels, a mean of diameter of 19.9 ± 12.5 μm, and double positive *foxc1b* + *acta2* covered vessels, a mean of 18.8 ± 12.0 μm (Fig. 5E and F). Thus, *foxc1b:EGFP* labels vSMCs on medium and large diameter vessels, which are distinct from pericyte-covered capillaries.

2.5. Intersectional expression of foxc1b and acta2 highlights the transcriptome of a unique head vSMC population

The transcriptome of vSMCs in early development has not been previously determined due to the lack of specific markers for vSMCs that exclude visceral smooth muscle. For instance, *acta2* is expressed in both vascular and visceral SMC populations. *foxc1b*, on the other hand is also expressed in a variety of neural crest derivatives in the head, but is not expressed in visceral smooth muscle. Thus, we used the intersection of *foxc1b* and *acta2* transgene expression for selective vSMC isolation using FACS. Isolated *acta2:EGFP* positive or *foxc1b:EGFP* + *acta2:mCherry* double positive cells, along with respective negative populations, were subjected to RNA-Seq (Figs. S7 and S8, Supplemental Table 1). There are 112 genes unique to the *acta2* dataset, 1076 genes unique to the *foxc1b* + *acta2* dataset, and 100 common genes between both datasets, with a $\log_2$-fold value changes of greater than 2 (Fig. S7). RNA-seq libraries from endothelial *kdrl:HRAS-mCherry* positive and negative cells were sequenced as a control. Consistent with a mural cell identity, both *acta2:EGFP* positive and *foxc1b:EGFP* + *acta2:mCherry* double positive cells show significantly enriched expression of known vascular smooth muscle genes, such as *acta2*, *tagln* and *fbln5*, when compared to the respective transgene negative populations (Fig. 6A and B). By contrast, neither population showed an enrichment for endothelial markers (*cdh5*, *pecam1*, *egfl7*; Fig. 6A–C). Interestingly, *myocardin* (*myocd*), a known transcriptional regulator of SMC differentiation in mammals (Du et al., 2003) only showed significant enrichment in *foxc1b:EGFP* + *acta2:mCherry* double positive cells (Fig. 6A and B), suggesting that intersectional transgene labeling improved detection of known mural cell genes. Indeed, multiple vSMC expressed genes show much higher levels of enrichment in *foxc1b:EGFP* + *acta2:mCherry* double positive cells when compared to negative cells, than the *acta2:egfp* positive population (Fig. 6D). As noted above, all but one of these genes (*myl9a*) failed to show any enrichment in endothelial cells (Fig. 6D). Gene Ontology analysis showed that the differentially expressed genes from both the *acta2* and *foxc1b* + *acta2* datasets are enriched in biological processes important in smooth muscle biology, including muscle contraction, regulation of vasoconstriction, blood circulation, and calcium ion homeostasis (Supplemental Table 2).

We performed whole mount *in situ* hybridization to validate the gene expression patterns of candidate vSMC genes. For this purpose, we

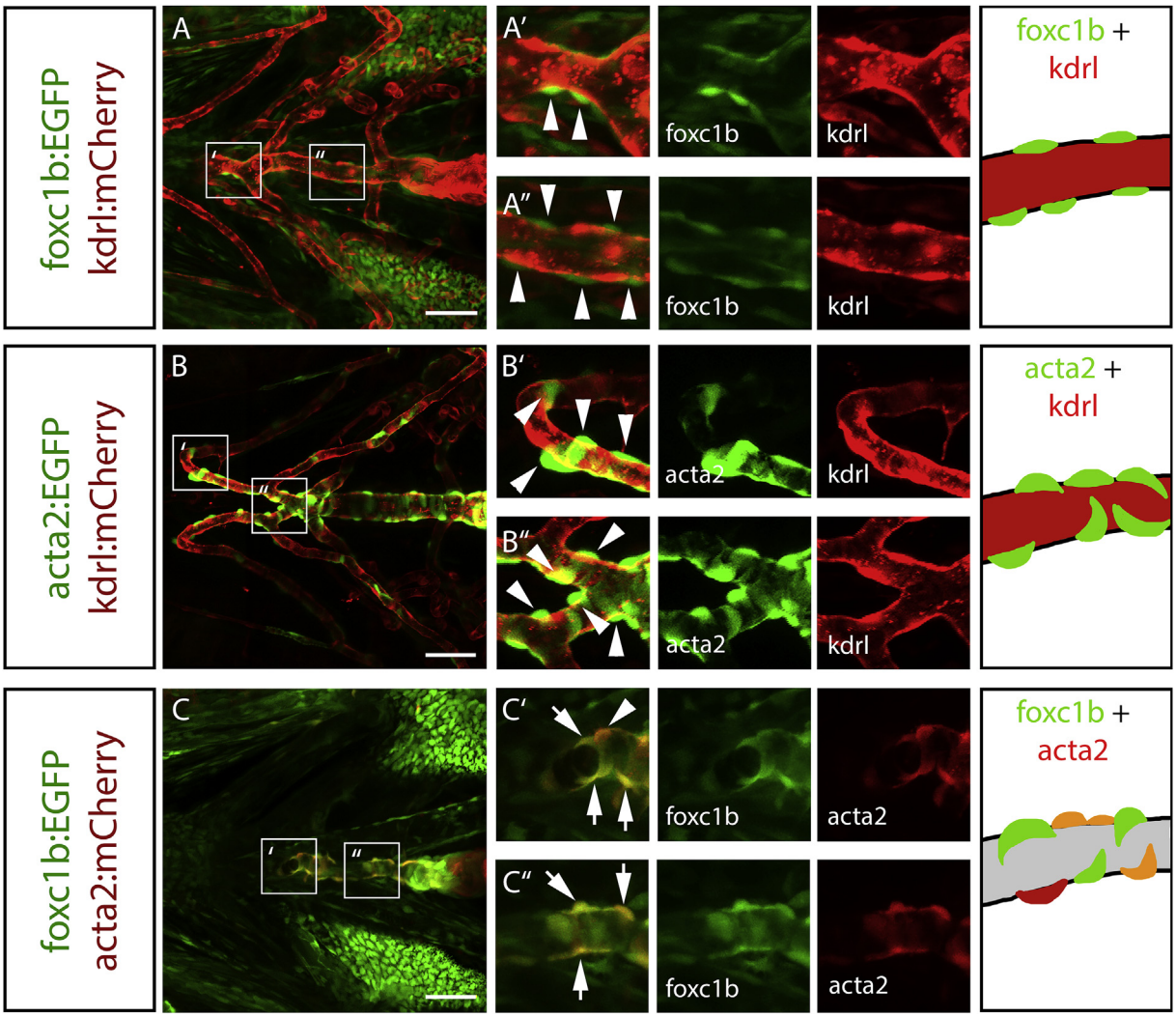

Fig. 3. *foxc1b* expressing perivascular cells in the embryonic ventral head co-express *acta2*. A) In ventral head vessels at 4 dpf, *foxc1b:EGFP* expressing cells are associated with, and surround, the endothelium (*kdrl:mCherry*) along the ventral aorta. B) Similarly, *acta2:EGFP* positive smooth muscle cells surround the *kdrl:mCherry* positive endothelium along the ventral aorta and aortic arch arteries. C) *foxc1b:EGFP* and *acta2:mCherry* are co-expressed along the ventral aorta. Schematics depict mural cell and endothelial marker expression matching the transgenes. Grey indicates presumptive endothelial patterns. Arrowheads represent marker-expressing mural cells. Arrows show co-expression of two smooth muscle cell markers. Scale bars represent 50 μm.

selected a subset of the top differentially expressed genes in both smooth muscle datasets (Figs. 6E and 7, Fig. S9), and compared expression to *acta2:EGFP*. In all cases, we observed expression in vSMCs of the aortic arch arteries where *foxc1b* and *acta2* are strongly expressed (Fig. 7). The transcripts are expressed in cells adjacent to the endothelium, suggesting they are expressed in mural cells (Fig. S9). Genes previously known to be involved in smooth muscle biology include *tagln, kcne4, cnn1b, lmod1b, desmb*, and *myl9a*. *tagln* (transgelin) is an actin binding protein commonly used as a smooth muscle marker. *knce4* (potassium voltage-gated channel subfamily E regulatory subunit 4) is an ion channel that regulates arterial tone. *cnn1b* (calponin 1b) is a known smooth muscle cell actin regulator. *lmod1b (*leiomodin) has functions in visceral smooth muscle, and *desmb* (desmin b) is an intermediate filament protein necessary for muscle function and is often used as a pericyte marker. *myl9a* (myosin light chain 9a) is a smooth muscle gene associated with contractility. Genes with some link to smooth muscle include *loxa* and *tpm4b*. *loxa* (lysyl oxidase) is associated with thoracic aortic aneurysms, while *tpm4b* (tropomyosin 4b) is an actin filament binding protein in vSMCs. Finally, *capn3b*, *pcolce2b* and *si:ch211-247i17.1* are examples of genes that do not have known roles in smooth muscle biology. *capn3b* (calpain 3b) is involved in HDL cholesteryl ester catabolism and limb-girdle muscular dystrophy, while *pcolce2b* (procollagen c-endopeptidase enhancer 2b) has no known role. *si:ch211-247i17.1* is a transcript with homology to an EF-hand calcium binding domain containing protein, but whose function is currently unknown in vertebrates. Together, these observations validate the enrichment for vascular smooth muscle genes using an intersectional approach to label vSMC populations and identify new genes involved in mural cell development and function.

2.6. *foxc1 genes are necessary for smooth muscle differentiation*

To assess the functional role of *foxc1* (*foxc1a* and *foxc1b*) in vSMC development, we developed CRISPR mutants for both genes. *foxc1b* and its paralog *foxc1a* have overlapping expression patterns and can compensate for each other (Skarie and Link, 2009; Topczewska et al., 2001; Xu et al., 2018). While we use *foxc1b* as a marker for vSMCs, *foxc1a* is highly enriched in our developmental vSMC transcriptome and there is strong co-expression of *foxc1a* in *foxc1b* + *acta2* double expressing vSMCs. We used crosses of *foxc1a*$^{+/-}$*; foxc1b*$^{+/-}$ compound heterozygotes (Fig. 8A and B). All embryos were heterozygous for the *acta2:EGFP* and *kdrl:mCherry* transgenes to visualize smooth muscle and the endothelium. As vSMC markers are first seen near the bulbus arteriosus and expand

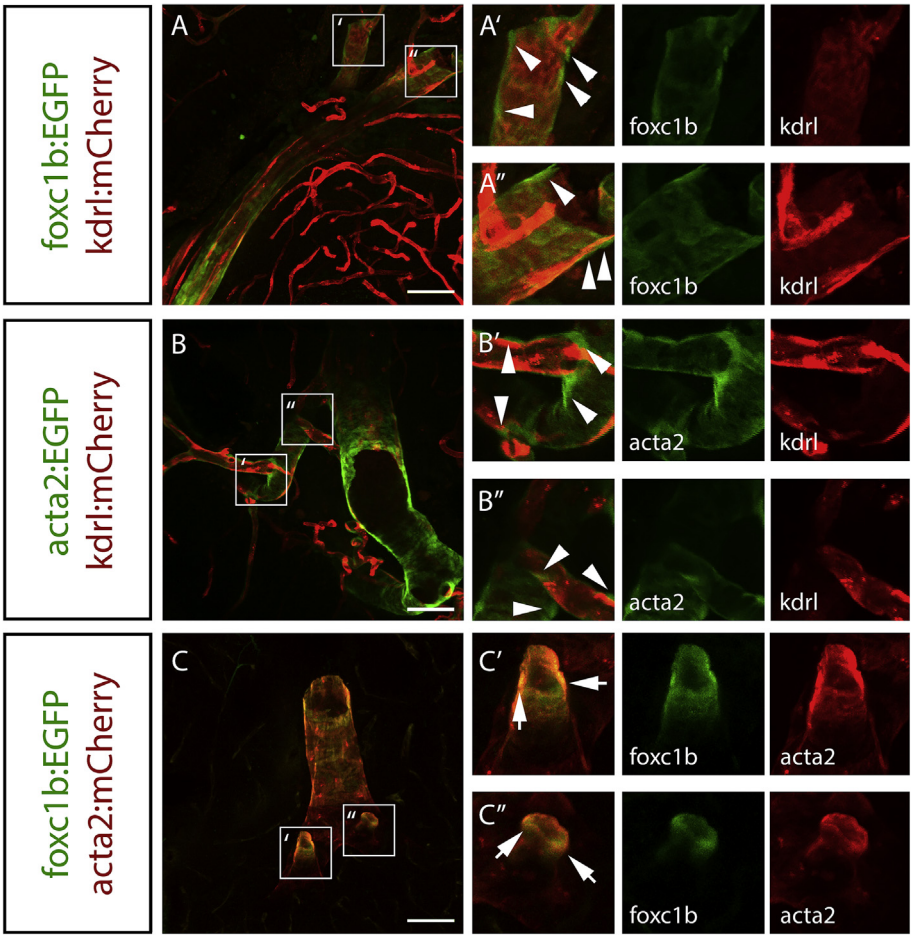

Fig. 4. *foxc1b* and *acta2* are co-expressed in vSMCs in the adult zebrafish brain. A) *foxc1b:EGFP* expressing cells are closely associated with endothelial cells (*kdrl:mCherry*) in the adult brain. Arrowheads point to mural cells associated with the endothelium. Arrows point to co-expression of two smooth muscle cell markers. B) *acta2:EGFP* expressing smooth muscle cells are closely associated with *kdrl:mCherry* expressing endothelial cells along large vessels of the brain. C) *foxc1b:EGFP* and *acta2:mCherry* are partially co-expressed in smooth muscle cells on brain vessels. Scale bars represent 50 μm.

rostrally, we measured the length of vSMC coverage on the ventral aorta extending rostrally from the bulbus as a measure of differentiation. At 3 dpf there was no significant difference in the length of smooth muscle coverage on the ventral aorta among mutant genotypes, and the ventral aorta has the same length among genotypes (Fig. S10, Supplemental Table 3). At 4 dpf, homozygous loss of *foxc1a*$^{-/-}$ has a strong effect on smooth muscle coverage with progressively stronger effects with increasing loss of *foxc1b* alleles on a *foxc1a* mutant background. Single mutant *foxc1a*$^{-/-}$; *foxc1b*$^{+/+}$ embryos are not significantly different from wild type, but *foxc1a*$^{-/-}$; *foxc1b*$^{+/-}$ and *foxc1a*$^{-/-}$; *foxc1b*$^{-/-}$ embryos have severely reduced smooth muscle coverage on the ventral aorta (Fig. 8C). At 4 dpf, the aorta is also significantly shorter in *foxc1a* mutants (Fig. 8D). We also note that *foxc1a* mutants initially develop circulation but develop progressive cardiac edema and circulatory insufficiency around 3 dpf. Measurements of the ventral aorta are difficult in these animals due to the presence of cardiac edema (Fig. S11; Supplemental Table 3). Our data suggest that *foxc1a and foxc1b* are critical for the early development of vSMCs, and cardiac function. Homozygous loss of *foxc1a* coupled with loss of one or two alleles of *foxc1b* has the strongest effect on vSMC development, but the converse is not true. Loss of two alleles of *foxc1b* and one allele of *foxc1a* has a wild type phenotype.

If *foxc1* is important for vSMC differentiation, loss of *foxc1* would be predicted to alter marker expression. Strikingly, expression of *acta2* and *pdgfrβ* are reduced in *foxc1a* mutants using hybridization chain reaction (HCR) *in situ* hybridization, as compared to wild type embryos (Fig. 8E). The levels of *acta2* and *pdgfrβ* are similar in *foxc1b* mutants, while both markers are absent in double *foxc1a*$^{-/-}$; *foxc1b*$^{-/-}$ mutants. We next examined the effects of loss of *foxc1a* and *foxc1b* on their own expression. Compared to wild type embryos, *foxc1a* mutants have a reduction of both *foxc1a* and *foxc1b* expression, while *foxc1b* mutants do not show visible reductions in either gene. In double *foxc1a*$^{-/-}$; *foxc1b*$^{-/-}$ mutants, the expression of both *foxc1a* and *foxc1b* are both decreased (Fig. 8E). To test whether loss of *foxc1* affected other smooth muscle genes, we assessed *myl9a* expression and found that loss of *foxc1a* has the strongest effect (Fig. 8G). These results for *myl9a* are similar to the expression of *acta2* in the mutants (Fig. 8E). Thus, *foxc1a* appears to control *foxc1b* expression and has a stronger effect on vSMC differentiation.

Since genetic *foxc1* mutants develop potentially confounding circulatory defects that may affect vSMC differentiation, we used a genetic ablation strategy where deletion of *foxc1b* expressing cells could be temporally controlled. We constructed *foxc1b:Gal4* or *acta2:Gal4* drivers that when combined with a *UAS-NTR:mCherry* reporter, and treated with the pro-drug metronidazole (MTZ), lead to the ablation of nitroreductase (NTR) expressing cells. *foxc1b* expressing cells are critical for vSMC differentiation as treatment of animals expressing *foxc1b:Gal4*; *UAS-NTR:mCherry* at 3 dpf before most vSMCs emerge resulted in a reduction in vSMCs on the ventral aorta (Fig. 9A and B). As a control, metronidazole treatment at 3 dpf of animals expressing *acta2:Gal4*; *UAS-NTR:mCherry* resulted in a similar loss of vSMCs on the ventral aorta (Fig. 9C and D). Control fish without the NTR construct do not have any patterning or vSMC coverage defects when treated with either dose of MTZ, suggesting that specific ablation of vSMCs leads to the phenotype (Fig. S12). Interestingly, MTZ ablation of *foxc1b* expressing cells also increases expression of *pdgfrβ* (Fig. 9F). The identity of these *pdgfrβ* expressing cells is unknown; however, they may be residual mural cells that were not ablated and have taken on a synthetic phenotype (Fig. 9E and F). Conversely, ablation of *acta2* expressing cells reduces both *acta2* and *pdgfrβ* expression along the ventral aorta (Fig. 9G and H). Finally, to address the temporal order of induction, ablation of *foxc1b* expressing cells result in a reduction of *foxc1b* (Fig. 9I and J), but *acta2* ablation does

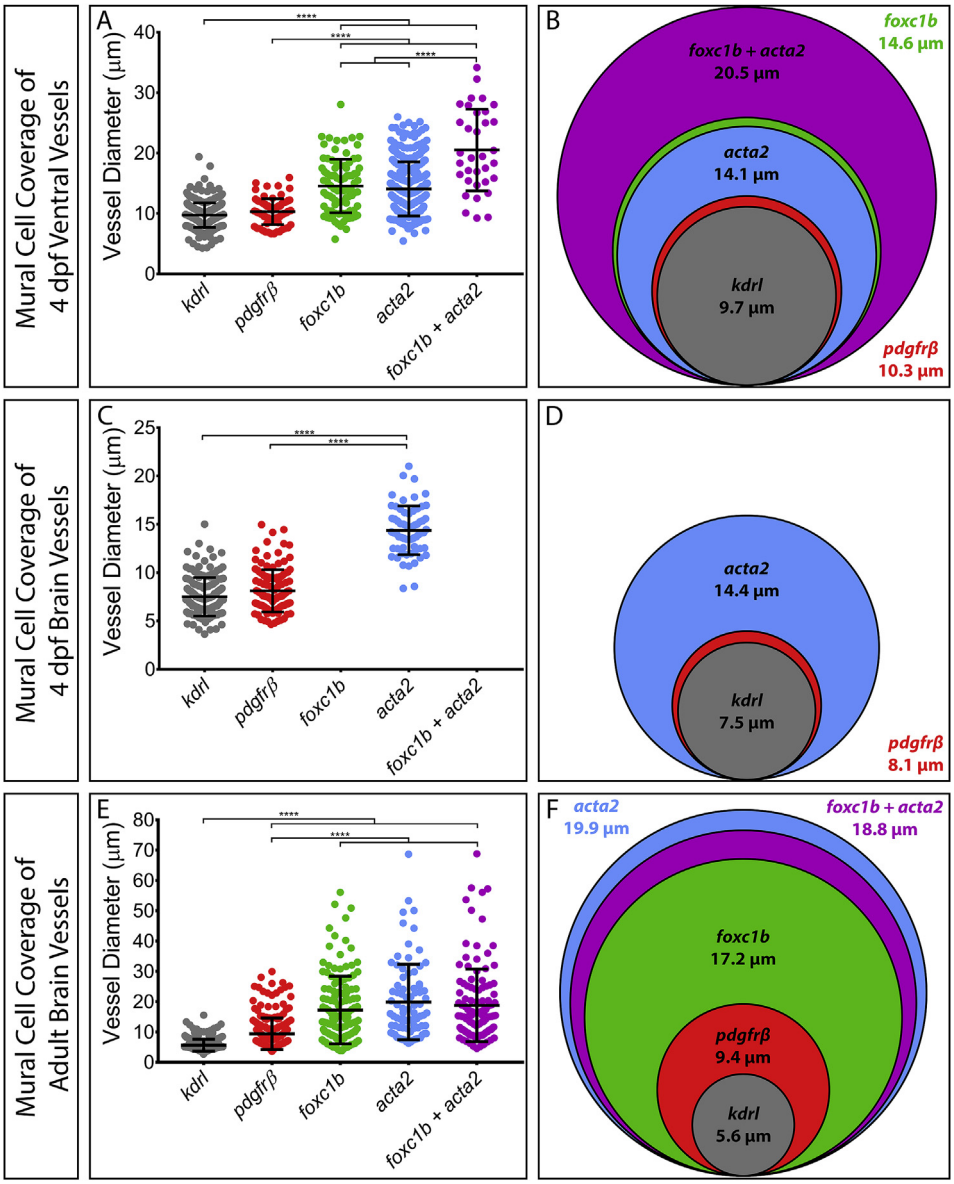

Fig. 5. *foxc1b* and *acta2* are co-expressed in some but not all vSMCs. A) Measurements of vessel diameter in naked vessels (vessels labelled by the endothelial *kdrl* transgene only) or vessels covered by different mural cells markers. Measurements of 4 dpf ventral head vessels: *kdrl* (9.7 ± 2.0 μm, n = 357), *pdgfrβ* (10.3 ± 2.1 μm, n = 75), *foxc1b* (14.6 ± 4.4 μm, n = 89), *acta2* (14.1 ± 4.5 μm, n = 308), and *foxc1b* + *acta2* (20.5 ± 6.8 μm, n = 34). B) Schematic of mean vessel diameter per condition with vessel sizes scaled relative to each other. C) Measurements of 4 dpf embryonic brain vessels: *kdrl* (7.5 ± 2.0 μm, n = 147), *pdgfrβ* (8.1 ± 2.2 μm, n = 119), and *acta2* (14.4 ± 2.5 μm, n = 63). D) Schematic of mean vessel diameter per condition with vessel sizes scaled relative to each other. E) Measurements of adult brain vessels: *kdrl* (5.6 ± 2.0 μm, n = 244), *pdgfrβ* (9.4 ± 5.2 μm, n = 238), *foxc1b* (17.2 ± 11.2 μm, n = 133), *acta2* (19.9 ± 12.5 μm, n = 83), and *foxc1b* + *acta2* (18.8 ± 12.0 μm, n = 126). F) Schematic of mean vessel diameter per condition with vessel sizes scaled relative to each other. **** = $p < 0.0001$, ANOVA with Tukey's multiple comparisons test.

not reduce *foxc1b* expression (Fig. 9K-L), suggesting *foxc1b* is expressed upstream of *acta2* in addition to being required for vSMC differentiation.

3. Discussion

We focus on the mechanisms of early development of vSMCs *in vivo* through functional studies of *foxc1*. We show that *foxc1b* is a marker of mesenchymal cells that differentiate to a smooth muscle morphology after they associate with endothelial tubes. Beyond being simply a marker of early vSMCs, we demonstrate defects in smooth muscle differentiation in *foxc1b* mutant fish. We also characterize the interplay between mural cell marker expression, vessel size, and use intersectional expression of two vSMC markers to identify an early head vSMC transcriptome.

3.1. Embryonic role of foxc1 in vascular development across species

foxc1b expression is limited to vSMCs and not expressed in the closely related pericyte lineage in zebrafish, despite expression of *Foxc1* in mouse brain pericytes (Siegenthaler et al., 2013; Zarbalis et al., 2007; Mishra et al., 2016). Instead we find that *foxc1b* (transgene and mRNA) is expressed in vSMCs in a similar expression pattern to *acta2*. The majority of these vSMCs are double positive for both *foxc1b* and *acta*. Single positive cells may have low expression levels of the other transgene and will eventually co-express both transgenes. It is currently unknown whether these cells which are *foxc1b:EGFP* negative; *acta2:mCherry* positive are *foxc1a* positive.

These differences in expression may reflect species differences between fish and mammals in expression and/or function of *foxc1*. We note that the smallest capillary vessel diameters, where pericytes are found, are set by the size of the erythrocyte (about 7–8 μm in diameter in humans and zebrafish) (Kulkeaw and Sugiyama, 2012) and are therefore comparable cross-species (Hartmann et al., 2015). *foxc1b* mRNA is also reportedly expressed within trunk endothelial cells during very early angiogenesis (Skarie and Link, 2009; Chen et al., 2017). In fish however, we do not see *foxc1b* expression in head or trunk endothelial cells at late embryonic stages (4 dpf) through adult (Prasitsak et al., 2015; Kume et al., 1998), as the gene is downregulated in later development.

The essential role of *foxc1* in smooth muscle in zebrafish is distinct from its role in other species. For instance, compound *Foxc1* and *Foxc2* mutant mouse vessels maintain *Acta2* positive smooth muscle coverage, although vessel morphology is altered such that vessels enlarge (Kume

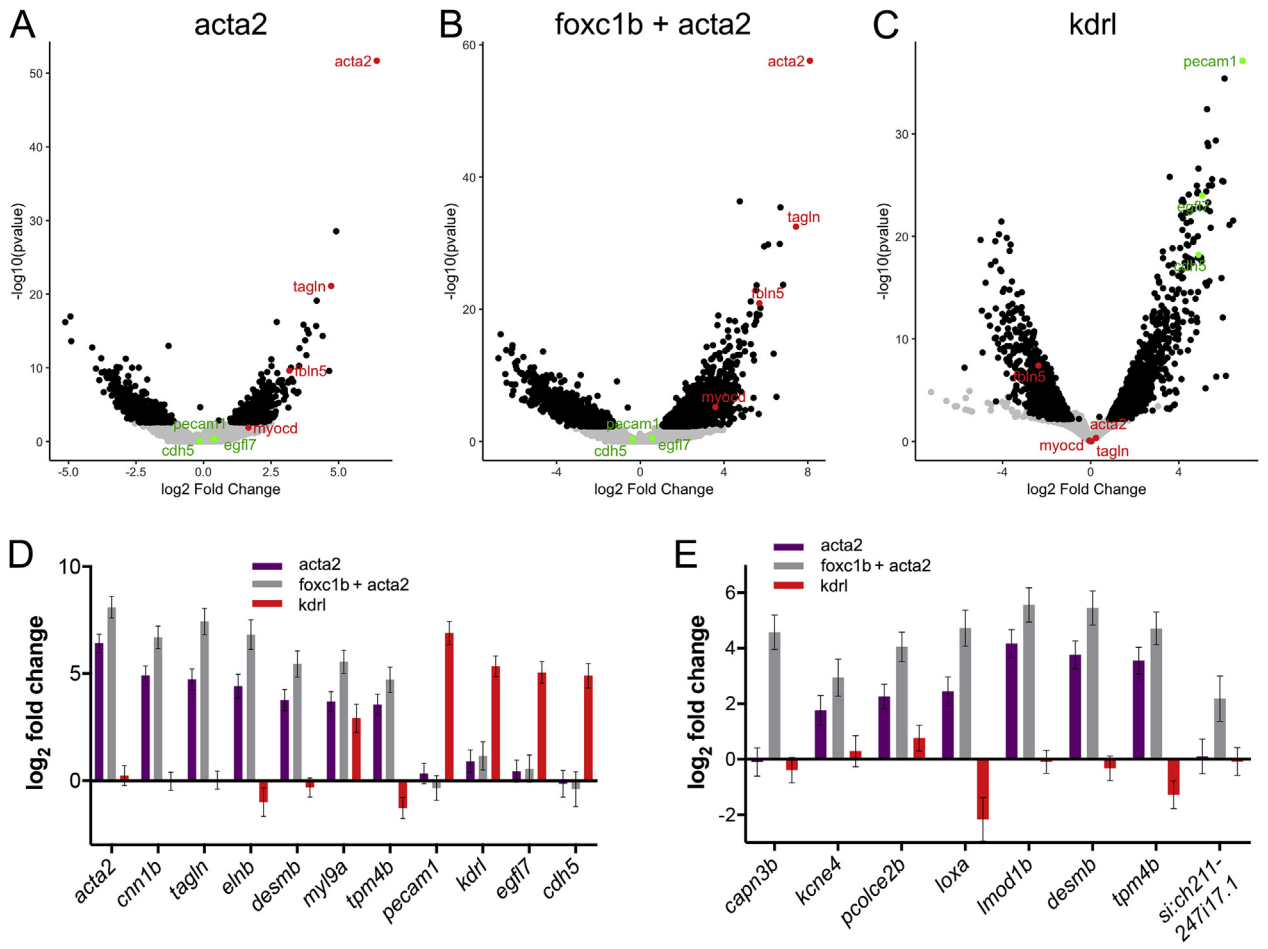

Fig. 6. Identification of gene expression in *foxc1*-positive embryonic smooth muscle and endothelial transcriptomes. A-C) Volcano plots for *acta2* positive smooth muscle (A), *foxc1b* + *acta2* positive smooth muscle (B), and *kdrl* positive endothelial (C) datasets. Representative smooth muscle genes are shown in red, whereas endothelial genes are shown in green. Black dots represent genes with significant changes (p adj < 0.05). D) Log_2 fold change in each dataset for genes indicated in the volcano plots. E) Log_2 fold change in each dataset for sample genes from Supplemental Table 1. Error bars in D and E are standard error.

et al., 2001). However, in fish we show that the loss of both *foxc1a* alleles and at least one *foxc1b* alleles blocks *acta2* positive smooth muscle differentiation on the ventral aorta. Whether *foxc1* acts during the migratory and/or differentiation stages of smooth muscle development is not yet known. Fox family members are known to play redundant roles in mice (Kume et al., 2001; Seo and Kume, 2006) and there is known genetic redundancy in zebrafish *foxc1* genes (Topczewska et al., 2001; Xu et al., 2018). It is likely that compensation by different Fox family members (or other transcription factors) in different species may explain the necessity of *foxc1* in vSMC differentiation in fish, but not in mouse.

3.2. *foxc1b promotes embryonic vascular smooth muscle cell differentiation*

Morpholino knockdown studies have shown that loss of *foxc1* reduces *acta2* expression, but not the role of *foxc1* in *acta2* expression. Our data here suggest that Foxc1 acts early in promoting vSMC differentiation. *foxc1b* function is required in mesenchymal precursors that will become *acta2* positive vSMCs. First, we observe mesenchymal expression of *foxc1b:EGFP* near vessels at 2 dpf and show how these cells undergo morphogenesis as they adhere to the endothelium and adopt a smooth muscle morphology. Secondly, *foxc1b* is expressed in vascular mural cells before the earliest *acta2* expression, and at later timepoints, the two genes are strongly co-expressed. Thirdly, loss of *foxc1* leads to a strong reduction in the number and the coverage by *acta2* positive vSMCs on the ventral aorta, both in genetic mutants and using a genetic ablation strategy. Taken together, these data suggest *foxc1b* expression and function is essential for mesenchymal precursors differentiate into *acta2* expressing vSMCs on the ventral aorta.

In mice, FOXC proteins are regulated by Sonic hedgehog (Shh), a signaling pathway driving mural cell differentiation (Lamont et al., 2010; Yamagishi et al., 2003). Given that *foxc1b* is expressed in neural crest (Seo et al., 2017; Koo and Kume, 2013; Seo and Kume, 2006; Inman et al., 2013), that lineage tracing of *sox10* expressing neural crest cells show they contribute to smooth muscle on the bulbus arteriosus and ventral aorta in fish (Cavanaugh et al., 2015; Mongera et al., 2013), and FOXC proteins are expressed in mural cells in mouse and fish (French et al., 2014; Siegenthaler et al., 2013; Kume et al., 2001), our data are consistent with previous models of the origin of the first vSMCs in the head of the embryo (Etchevers et al., 2001; Wang et al., 2014; Cavanaugh et al., 2015; Mongera et al., 2013; Calloni et al., 2007).

3.3. *Identification of an embryonic vascular smooth muscle transcriptome*

We show that cell sorting using the intersectional expression of two markers is a powerful strategy to enrich the population of vSMCs. Within the vSMC transcriptomes, we observe strong expression of expected genes such as *acta2, tagln, tpm4b,* and *desmb*. Other muscle related genes (for example, myosins, ion channels, and receptors) are present, and we also identify many genes which are novel, denoted only by chromosomal location that should be explored for functional roles in vSMCs.

Our vSMC transcriptome is unique in profiling vSMCs as they first

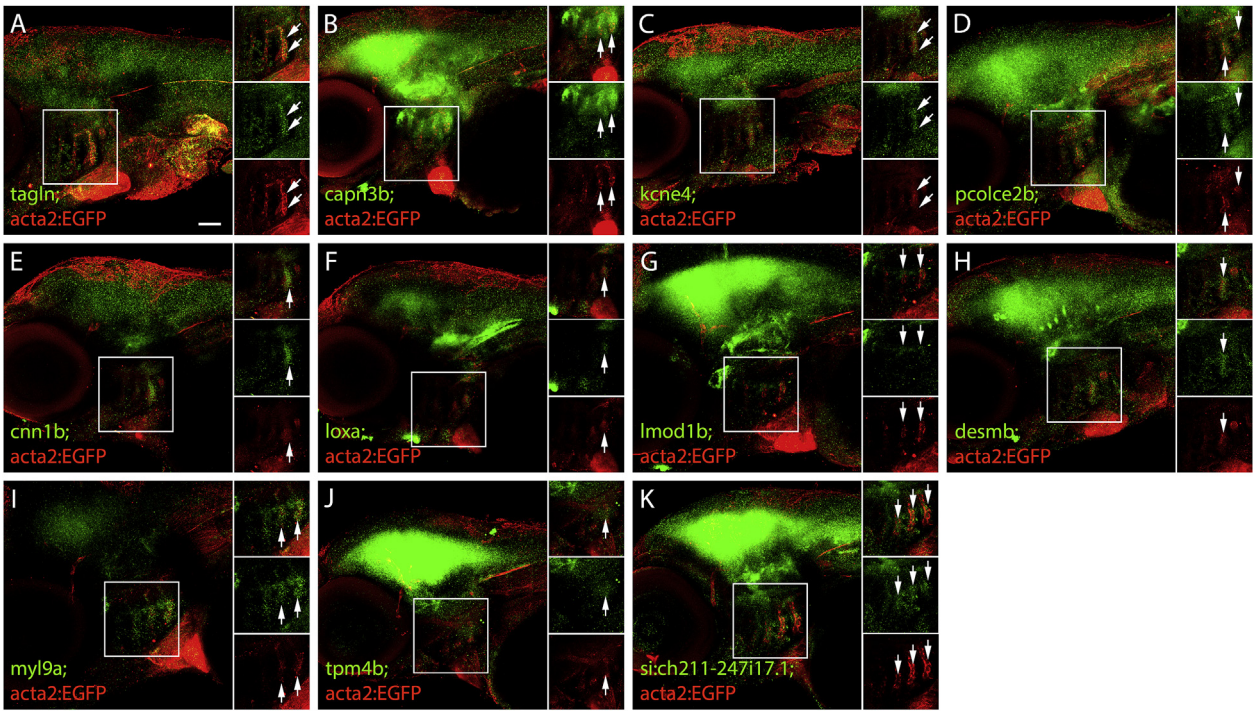

Fig. 7. Expression of genes with enriched expression in the embryonic vSMC transcriptome. Gene expression from *in situ* hybridization in laterally mounted 4 dpf embryos. Gene of interest mRNA is depicted in green, with αGFP antibody (red) detecting *acta2:EGFP* transgenic expression in smooth muscle cells. Arrows depict co-expression of gene of interest mRNA with *acta2:EGFP* expression. A) *tagln* is expressed in the aortic arch arteries, and co-expressed with *acta2:EGFP*. B) *capn3b* expressed in the aortic arch arteries and brain. C) *kcne4* is lowly expressed in the aortic arch arteries. D) *pcolce2b* is expressed in the aortic arch arteries and the brain. E) *cnn1b* is expressed in the aortic arch arteries. F) *loxa* is expressed in the aortic arch arteries, the bulbus arteriosus, and the ventral brain. G) *lmod1b* is expressed in the aortic arch arteries and brain. H) *desmb* is expressed in the aortic arch arteries, and in punctate patterns in the brain. I) *myl9a* is expressed in the aortic arch arteries. J) *tpm4b* is expressed in the brain and lowly expressed in the aortic arch arteries. K) *si:ch211-247i17.1* is expressed in the aortic arch arteries and brain. Scale bar represents 50 μm.

differentiate in early development at 4 dpf, near the onset of smooth muscle marker expression. Previous mouse mural cell transcriptomes use late embryonic, postnatal or adult mice (He et al., 2016; Vanlandewijck et al., 2018; Lee et al., 2015). The transcriptomes of mouse visceral smooth muscle (Lee et al., 2015), and single cell transcriptomes of the brain vasculature to identify endothelial, smooth muscle, pericyte, fibroblast, and astrocyte cells (Vanlandewijck et al., 2018) are complementary to our data. Developmental pericyte transcriptomes are also complementary to our data. A *pdgfrβ* expressing cell transcriptome at E17.5 (Bondjers et al., 2006), was embryonic, but is at a stage multiple days after the onset of classic mural cell marker expression in embryonic mice (Lindahl et al., 1997; Hellström et al., 1999). In postnatal mice, *pdgfrβ* and *ng2* double positive pericytes have been sequenced (He et al., 2016) and compared to four other pericyte studies, resulting in a pooled brain mural cell transcriptome.

Comparing our transcriptomes to the previously published mouse smooth muscle transcriptome datasets (Vanlandewijck et al., 2018; Lee et al., 2015), we find many genes shared between the datasets, as expected. These include the common mural cell markers *acta2, tagln, desmb, cnn1b, myl9a,* and *mylh11a* that are also observed in murine colonic and jejunal smooth muscle transcriptomes (Lee et al., 2015), and arterial, arteriolar, or venous smooth muscle cell transcriptomes (Vanlandewijck et al., 2018). As our *acta2:EGFP* transcriptome will contain transcripts from vascular and visceral smooth muscle, it is expected that we find many general vSMC genes. However, *foxc1b:EGFP* + *acta2:mCherry* represents an enriched vascular SMC transcriptome. Interestingly, there are more than 20 uncharacterized genes common to both the *acta2* and foxc1b + acta2 datasets, almost 50 uncharacterized genes in the *acta2* dataset, and more than 250 uncharacterized genes in the *foxc1b* + *acta2* datasets. These uncharacterized genes warrant further investigation for functional roles in smooth muscle. Expression analysis of *si:ch211-247i17.1*, a predicted calcium EF-hand protein in our study shows strong vSMC expression. Functional analysis of this and other unstudied and annotated genes has the potential to reveal new pathways in vSMC differentiation.

Our data on early migration, differentiation and transcriptional profile of vSMCs will allow for a better understanding of how early vSMCs migrate and undergo differentiation. Our data suggest that *foxc1* is a necessary transcription factor for differentiation of the head vSMC lineage. The identity of *foxc1* targets and whether it cooperates with other transcription factors to drive vSMC differentiation will be an area of immense interest for future experiments.

4. Materials and methods

4.1. Ethics, husbandry, and strains

Zebrafish husbandry was performed following standard protocols (Westerfield, 1995). All procedures were approved by the University of Calgary Animal Care Committee, the University of Massachusetts Medical School IACUC, and the University of Alberta Animal Care and Use Committee-Biological Sciences (ACUC-BioSci). Zebrafish strains/transgenic lines include: wild type Tupfel long fin (TL), *Tg(kdrl:mCherry)*^{ci5} (Proulx et al., 2010), *Tg(kdrl:EGFP)*^{la116} (Choi et al., 2007), *Tg(kdrl:HRAS-mCherry)*^{s896} (Chi et al., 2008), *Tg(acta2:EGFP)*^{ca7} (Whitesell et al., 2014), *Tg(acta2:mCherry)*^{ca8} (Whitesell et al., 2014), *TgBAC(pdgfrβ:Gal4FF*^{ca42} (Ando et al., 2016); *UAS-NTR:mCherry)*^{c264} (Davison et al., 2007), hereafter *Tg(pdgfrβ:mCherry)*, *Tg(-5.0kbfoxc1-b:EGFP)*^{mw44} (Miesfeld and Link, 2014).

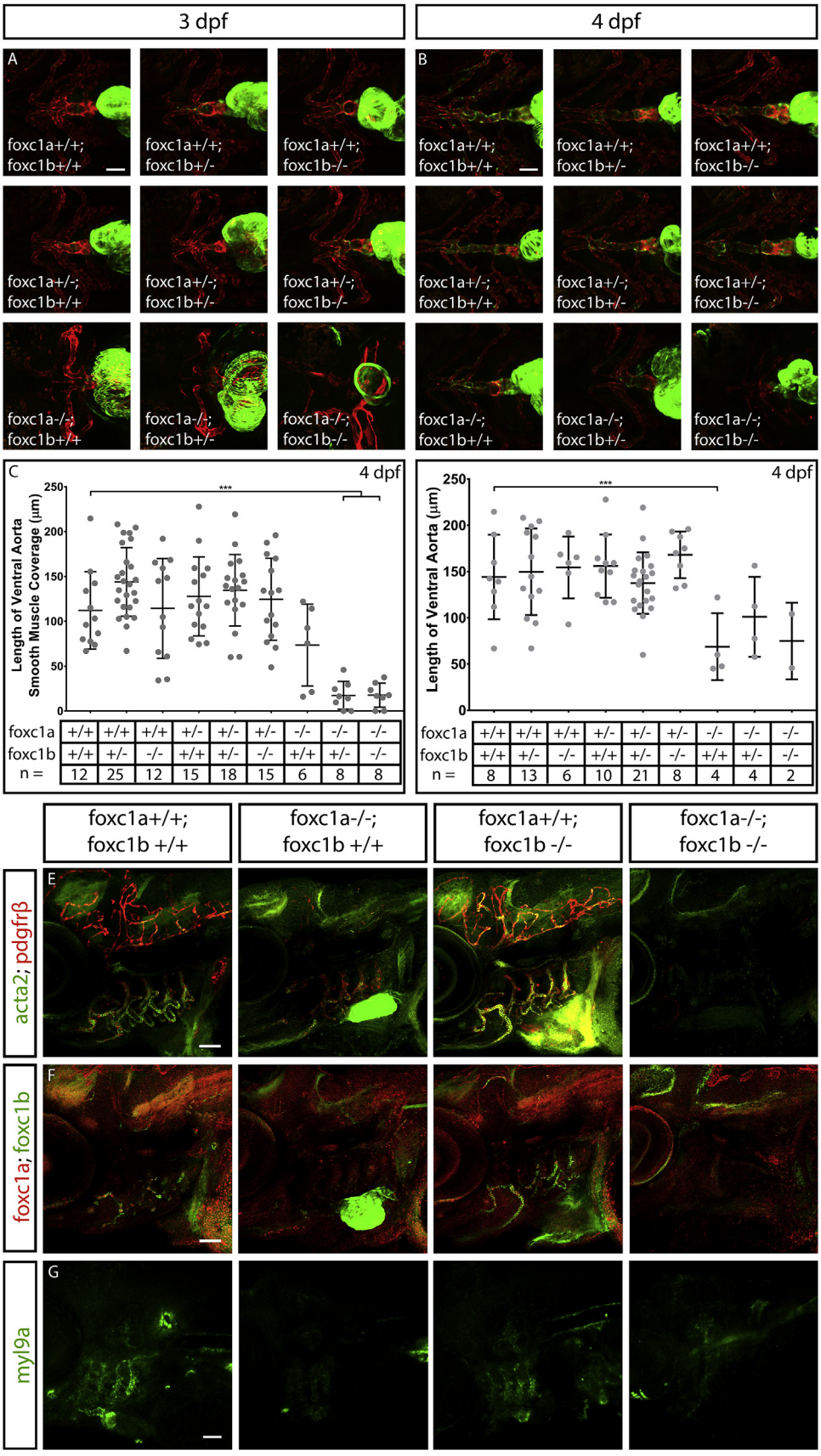

Fig. 8. Necessity of *foxc1* for embryonic head vSMC development. A) Ventral images of 3 dpf embryos depicting ventral aorta (red) and smooth muscle coverage (green) in *foxc1a/foxc1b* mutant genotypes. B) Ventral images of 4 dpf embryos depicting ventral aorta (red) and smooth muscle coverage (green) in *foxc1a/foxc1b* mutant genotypes. Genotypes are listed in each corresponding panel. C) At 4 dpf, the length of smooth muscle coverage on the ventral aorta is reduced *foxc1a*$^{-/-}$ mutants. D) At 4 dpf, the length of the ventral aorta is significantly reduced in *foxc1a*$^{-/-}$ mutants. E) Mural cell markers *acta2* and *pdgfrβ* have reduced expression with the loss of *foxc1a*, and a stronger effect with the combined loss of *foxc1a* and *foxc1b*, compared to wildtype and loss of *foxc1b* alone at 4dpf. F) Compared to wildtype embryos, expression of *foxc1a* and *foxc1b* are both decreased in *foxc1a mutants*. The combined loss of both *foxc1a* and *foxc1b* results in a lack of expression of *foxc1a* or *foxc1b*. G) *myl9a* expression in the aortic arch arteries is reduced with the loss of *foxc1a*, either in *foxc1a* mutants, or in combined *foxc1a/foxc1b* mutants. *** = $p < 0.0001$, ANOVA with Dunnett's multiple comparisons test. Scale bar represents 50 μm.

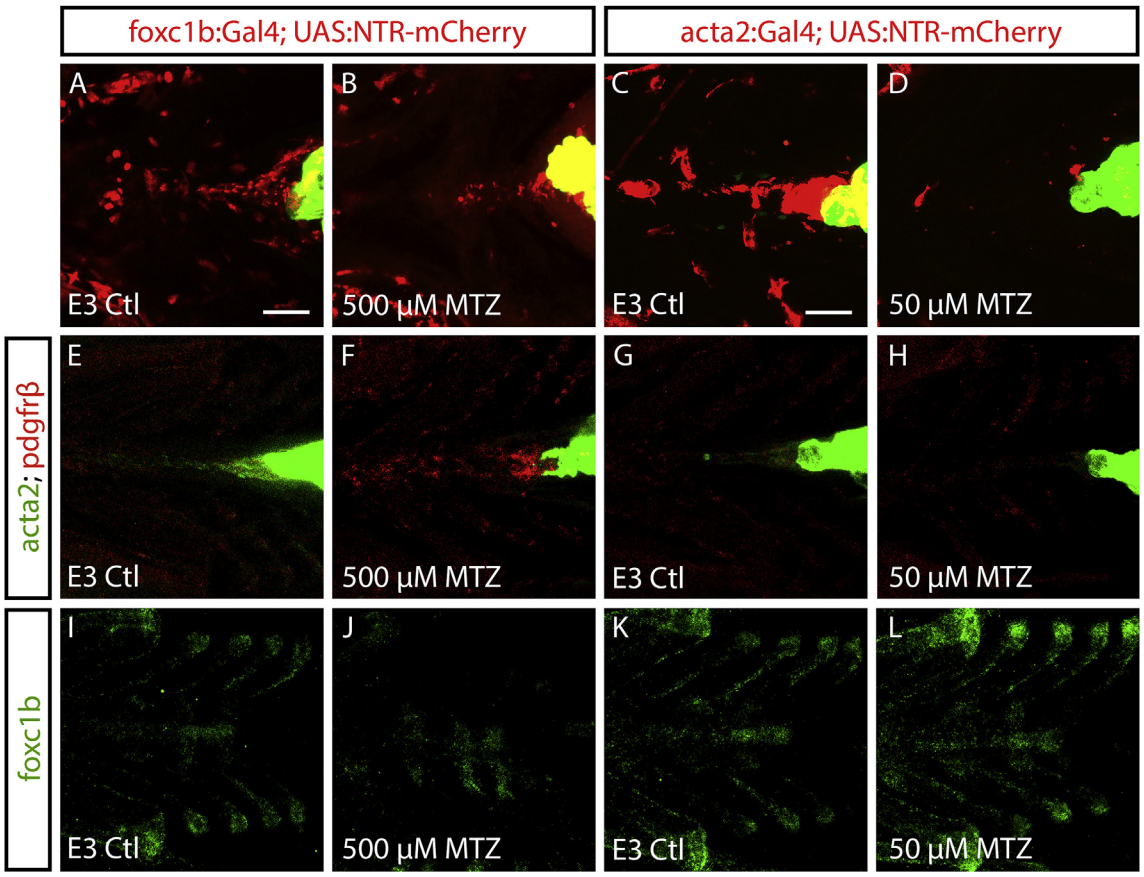

Fig. 9. *foxc1* acts upstream of *acta2* in vSMC differentiation. A-D) Ablation of *foxc1b* and *acta2* positive cells using Metronidazole (MTZ) from 3 to 4 dpf. Embryos are heterozygous for *foxc1b*- or *acta2:Gal4* and *UAS:NTR-mCherry*. Ventral views show smooth muscle coverage along the ventral aorta in controls (A and C), but largely absent in MTZ treated embryos (B, D). E-F) Ventral views of mural cell marker mRNA (*acta2* and *pdgfrβ)* in *foxc1b:Gal4; UAS:NTR-mCherry* embryos show a reduction in *acta2* and increase in *pdgfrβ* in MTZ treated embryos (F) versus controls (E). G-H) Expression of *acta2* is reduced in MTZ treated *acta2:Gal4; UAS:NTR-mCherry* embryos versus controls, while *pdgfrβ* expression is unchanged. I-L) Expression of *foxc1b* mRNA is reduced in MTZ treated *foxc1b:Gal4; UAS:NTR-mCherry* embryos compared to controls, while *foxc1b* mRNA is unchanged in controls and MTZ treated *acta2:Gal4; UAS:NTR-mCherry* embryos. Green hearts in A-H are due to the transgenesis marker (*myl7:EGFP*). Scale bar represents 50 μm.

4.2. Generation of mutant and transgenic strains

Generation of *foxc1a*^{ua1017} and *foxc1b*^{ua1018} CRISPR mutant strains each required two guide RNAs, produced by cloning into pDR274 (Addgene, #42250), followed by in vitro transcription using the MAXIscript T7 Transcription kit (Ambion, Cat. No. AM1312). *foxc1a*^{ua1017} target sequences (5′-3′) were AACTCGCTGGGAGTTGTGCC and CCGCCGCCGGAGGGGGGTACACC. *foxc1b*^{ua1018} target sequences (5′-3′) were GGCGTTGTGCCTTATATCCC and CGACCGGTGGTGGATATACC (Umali et al., 2019).

Cas9 mRNA was synthesized from pMLM3613Cas9 (Addgene, #42251) using a mMESSAGE mMACHINE T7 Transcription kit (Ambion, Cat. No. AM1344), followed by a Poly-A Tailing Kit (Ambion, AM1350). Injections were standardized using 30 ng/μl per gRNA and 300 ng/μl Cas9. Injected fish (P0) were outcrossed and embryos were screened using HRM (Qiagen, Rotor-Gene Q). Mutations were cloned and sequenced from genomic DNA and RNA.

Tg(acta2:Gal4FF)^{ca62}, and *Tg(foxc1b:gal4FF)*^{ca72} were generated using the Tol2Kit (Kwan et al., 2007) and the *acta2* promoter-enhancer (Whitesell et al., 2014) or *-5.0foxc1b* promoter (Miesfeld and Link, 2014), in front of pME:gal4FF and a p3E:polyA in the Tol2 backbone containing *myl7:EGFP* as a transgenic marker (pDESTTol2CG2). *TgBAC(pdgfrβ:Gal4FF*^{ca42}*)* was generated by a new injection of the described BAC (Ando et al., 2016). Positive F0 founders were bred to the F1 and F2 generation on the *Tg(UAS-NTR:mCherry)*^{C264} background.

4.3. Sectioning, imaging and image analysis

Confocal images were collected on either a Zeiss LSM 700 or an Olympus FV1200 confocal microscope. Embryos were mounted in 0.8% low melt agarose on glass bottom dishes (MatTek, Ashland, MA, Cat. No. P50G-0-30-F), and were incubated in a heated chamber with the addition of 0.4% Tricaine (Sigma, Cat. No. A5040) for restraint. Representative images are shown.

Adult zebrafish brains (0.5–1.5 years old) were dissected and fixed overnight in 4% PFA/1x PBS. Brains were washed in PBS (3 × 5 min) before being mounted in a 55 °C gelatin solution (15% w/v). Coronal vibratome sections were cut on a Leica Vibratome VT1000S at a thickness between 150 and 300 μm.

Wholemount imaging of stained samples was conducted with a Zeiss Stemi SV11 microscope, with a Zeiss HR camera. Stained wholemount embryos were sectioned at 8 μm after mounting in JB4 resin (Polysciences, Warrington, PA). Sections were imaged on a Zeiss Axio Imager.Z1 microscope with an AxioCam ICc5 camera (Zeiss).

Vessel diameter measurements were measured from confocal images using FIJI/ImageJ (Schindelin et al., 2012). Diameters were measured from the external diameter of the endothelium, away from nuclei of mural and endothelial cells. Seven measurements were taken for each sample where possible. Ventral head measurements were taken from the ventral aorta and the aortic arch arteries. In the brain, measurements were predominantly taken from the internal carotid artery (smooth muscle) and central arteries (pericytes). Measurements represent mean

vessel diameter ± standard deviation in micrometers.

4.4. In situ hybridization and antibody staining

in situ hybridization (colorimetric and fluorescent) was performed using the method of Lauter et al., 2011) (Lauter et al., 2011), with the following modifications. Embryos were permeabilized in 2% H_20_2/methanol for 20 min and depigmented in 3% H_20_2/0.5% KOH in water for 10 min. Proteinase K permeabilization was at 10 μg/ml for 1 h for 4 dpf embryos. EGFP was detected with 1:500 mouse αGFP (JL-8, BD Clontech/Takara Bio USA) and the Vectastain ABC Kit (Vector Laboratories, Burlingame CA, USA), using 1:400 αDIG POD Fab fragment (Roche, Cat. No. 11 207 733 910) and FAM (ThermoFisher, Cat. No. C1311) for green fluorescent probe signal, or mouse αGFP (1:500, JL-8, BD Clontech/Takara Bio USA) and Alexa555 goat α mouse fluorescent secondary antibody (1:500, ThermoFisher, Cat. No. A21422). Primers for *in situ* hybridization are listed in Supplemental Table 4.

HCR (hybridization chain reaction) *in situ* hybridization was performed using the method of Choi et al, 2018) (Choi et al., 2018). 4 dpf embryos were used to assess *acta2* (NM_001177452.1; Amplifier B1; Fluorophore: Alexa488), *pdgfrβ* (NM_001177452.1; Amplifier B4; Fluorophore: Alexa594), *foxc1a* (NM_001177452.1; Amplifier B2; Fluorophore: Alexa647), and *foxc1b* (NM_001177452.1; Amplifier B3; Fluorophore: Alexa546) probes (Molecular Instruments, Inc., Los Angeles CA, USA).

4.5. FACS & RNA isolation

The protocol for single cell dissociation was based upon Rougeot et al. 2014. 300 *acta2:EGFP* and 300 *foxc1b:EGFP* + *acta2:mCherry* (4 dpf) fish were anesthetized with 0.4% Tricaine (Sigma) and pooled. Embryos were treated for 15 min with calcium-free Ringers Solution and triturated 15 times. Dissociation Solution was added and triturated 10 times before placing in a 28.5 °C water bath with shaking at 60 rpm and periodic trituration for 1 h. The reaction was stopped, centrifuged and resuspended in Dulbecco's Phosphate-Buffered Saline (GIBCO by Life Technologies; REF 14040–133), centrifuged and resuspended in fresh Resuspension Solution. The single cell suspension was filtered with 75 μm, followed by 35 μm filters. Cells were then sorted with a BD FACSAria III (BD Bioscience, San Jose, USA) and collected into a collection solution. RNA Isolation of sorted cells was performed using the Trizol method (Ambion by Life Technologies; Carslbad CA, USA; Cat No. 15596026). For analysis of *kdrl:HRAS-mCherry* cells, larvae bearing transgene were anesthetized at 5 dpf, dissociated into single cell suspensions, fixed, and subjected to fluorescence activated cell sorting (FACS) by the University of Massachusetts Medical School Flow Cytometry Core, as described previously (Quillien et al., 2017).

4.6. Next generation sequencing and bioinformatics

Library preparations used the REPLI-g Single Cell Kit (Cat. No. 150343, Qiagen) for paired end sequencing of 4 dpf samples, using an Illumina NextSeq Platform. 4 dpf samples were: *acta2:EGFP*$^+$, *acta2:EGFP*$^-$; and *foxc1b:EGFP*$^+$ + *acta2:mCherry*$^+$, *foxc1b:EGFP*$^-$ + *acta2:mCherry*$^-$). RNA isolation and library preparation for *kdrl:HRAS-mCherry* positive and negative cell populations was handled as previously reported (Quillien et al., 2017).

The sequencing depth for *acta2:EGFP* positive samples averaged 54.8 million reads and 60.9 million reads for the negative population. The sequencing depth for *foxc1b:EGFP* + *acta2:mCherry* double positive samples averaged 59.7 million reads and 61.5 million reads for the double negative population. The sequencing depth for *kdrl:HRAS-mCherry* samples averaged 52.7 million reads for the positive population and 39.1 million reads for the negative population.

Paired-end reads were aligned to 26 chromosomes and 967 primary assembly scaffolds of the zebrafish genome GRCz11, with star_2.5.3a (Dobin et al., 2013). Aligned exon fragments with mapping quality higher than 20 were counted toward gene expression with featureCounts_1.5.2 (Liao et al., 2014). Normalization and differential expression (DE) analysis was performed with DESeq2_1.20.0 (Love et al., 2014). For DE analysis, the original DESeq2 shrinkage estimator was used to estimate log2 fold change (LFC) for each comparison. False discovery rate (FDR < 0.05) and $|LFC| > 1$ was used as a cut-off to identify significantly enriched genes. Parameters: GTF: GCF_000002035.6_GRCz11_genomic.ucsc.primary.gff. Genome: danRer11.primary.fa.

For gene ontology analysis and biological processes enriched in the datasets, see Supplemental Table 2. PANTHER analysis was performed with PANTHER 13.1, Gene Ontology version: 1.2, Gene Ontology annotations: 2018-08-09, Reference Proteome: 2017_04. Analysis used the *Danio rerio* genome, a statistical overrepresentation test with default settings and PANTHER GO-Slim Biological Process, and the test type was Fisher's Exact with FDR multiple test correction {Mi H PANTHER}.

4.7. Smooth muscle quantification and ablation experiments

Images of heterozygote transgenic *acta2:EGFP; kdrl:mCherry* fish were analyzed in FIJI/ImageJ (Schindelin et al., 2012). Measurements were recorded from the point where the bulbus arteriosus merges with the ventral aorta to the distal tip of smooth muscle expression on the ventral aorta or to the bifurcation point of the ventral aorta, whichever was shorter (Isogai et al., 2001). Measurements are presented in Supplemental Table 3.

Ablation of *foxc1b* + or *acta2*+ positive was performed using *foxc1b:Gal4;UAS-NTR:mCherry* or *acta2:Gal4;UAS-NTR:mCherry* zebrafish. Embryos were treated with Metronidazole (MTZ, Sigma-Aldrich Cat. No. M3761) from 3 to 4 dpf, with *foxc1b:Gal4;UAS-NTR:mCherry* fish receiving 500 μM MTZ and *acta2:Gal4;UAS-NTR:mCherry* fish receiving 50 μM MTZ.

Data availability

Complete methods are available in the supplementary methods. RNA sequencing data is available from the Gene Expression Omnibus (GEO) site (www.ncbi.nlm.nih.gov/geo/) with accession number GSE119718. A key resources table (KRT) is available in Table 2.

Acknowledgments:

We would like to thank Charlene Watterston, Jasper Greysson-Wong, Nabila Bahrami, and Danielle Blackwell, in addition to the laboratory of Dr. Peng Huang for their helpful comments on the project and paper. We would like to thank the members of the Flow Cytometry core facility and the Alberta Children's Hospital Research Institute (ACHRI) Genomics Platform at the University of Calgary.

Appendix A. Supplementary data

Supplementary data to this article can be found online at https://doi.org/10.1016/j.ydbio.2019.06.005.

Funding

This work was funded by Natural Sciences and Engineering Research Council of Canada Discovery Grant (RGPIN 06360-2014) to SJC. SJC was a Canada Research Chair Tier II and an Alberta Innovates Health Solutions Senior Scholar. TRW was funded by scholarships from the Alberta Innovates Health Solutions Graduate Studentship, the Kertland Family Doctoral Scholarship in Vascular Biology, and an Achievers in Medical Sciences Scholarship from the University of Calgary. AW was funded by Natural Sciences and Engineering Research Council of Canada Discovery Grant (RGPIN 298371). OJL was funded by the Canadian Institutes of Health Research (MOP-133658) and the Women and Children's Health

Research Institute. NDL was funded by the National Institutes of Health – National Heart, Lung, and Blood Institute (R35HL140017).

References

Abrams, J., et al., 2016. Graded effects of unregulated smooth muscle myosin on intestinal architecture, intestinal motility and vascular function in zebrafish. Dis. Model. Mech. 9, 529–540.

Ando, K., et al., 2016. Clarification of mural cell coverage of vascular endothelial cells by live imaging of zebrafish. Development 143, 1328–1339.

Armulik, A., Genové, G., Betsholtz, C., 2011. Pericytes: developmental, physiological, and pathological perspectives, problems, and promises. Dev. Cell 21, 193–215.

Avasarala, J.R., Jones, J.R., Rogers, C.R., 2018. Forkhead box C1 gene variant causing glaucoma and small vessel angiopathy can mimic multiple sclerosis. Mult. Scler. Relat. Disord. 22, 157–160.

Baron-Menguy, C., Domenga-Denier, V., Ghezali, L., Faraci, F.M., Joutel, A., 2017. Increased Notch3 activity mediates pathological changes in structure of cerebral arteries. Hypertension 69, 60–70.

Bergers, G., Song, S., 2005. The role of pericytes in blood-vessel formation and maintenance. Neuro Oncol. 7, 452–464.

Berthiaume, A.-A., et al., 2018. Dynamic remodeling of pericytes in vivo maintains capillary coverage in the adult mouse brain. Cell Rep. 22, 8–16.

Birbrair, A., et al., 2017. How plastic are pericytes? Stem Cells Dev. scd. 2017 https://doi.org/10.1089/scd.2017.0044, 0044.

Bondjers, C., et al., 2006. Microarray analysis of blood microvessels from PDGF-B and PDGF-Rbeta mutant mice identifies novel markers for brain pericytes. FASEB J. 20, 1703–1705.

Calloni, G.W., Glavieux-Pardanaud, C., Le Douarin, N.M., Dupin, E., 2007. Sonic Hedgehog promotes the development of multipotent neural crest progenitors endowed with both mesenchymal and neural potentials. Proc. Natl. Acad. Sci. U. S. A. 104, 19879–19884.

Carmeliet, P., Jain, R.K., 2011. Molecular mechanisms and clinical applications of angiogenesis. Nature 473, 298–307.

Cavanaugh, A.M., Huang, J., Chen, J.N., 2015. Two developmentally distinct populations of neural crest cells contribute to the zebrafish heart. Dev. Biol. 404, 103–112.

Chen, X., Gays, D., Milia, C., Santoro, M.M., 2017. Cilia control vascular mural cell recruitment in vertebrates. Cell Rep. 18, 1033–1047.

Chi, N.C., et al., 2008. Foxn4 directly regulates. Genes Dev. 734–739. https://doi.org/10.1101/gad.1629408.734.

Choi, J., et al., 2007. FoxH1 negatively modulates flk1 gene expression and vascular formation in zebrafish. Dev. Biol. 304, 735–744.

Choi, H.M.T., et al., 2018. Third-generation *in situ* hybridization chain reaction: multiplexed, quantitative, sensitive, versatile, robust. Development 145, 165753.

Craggs, L.J.L., Yamamoto, Y., Deramecourt, V., Kalaria, R.N., 2014. Microvascular pathology and morphometrics of sporadic and hereditary small vessel diseases of the brain. Brain Pathol. 24, 495–509.

Craggs, L.J.L., Fenwick, R., Oakley, A.E., Ihara, M., Kalaria, R.N., 2015. Immunolocalization of platelet-derived growth factor receptor-β (PDGFR-β) and pericytes in cerebral autosomal dominant arteriopathy with subcortical infarcts and leukoencephalopathy (CADASIL). Neuropathol. Appl. Neurobiol. 41, 557–570.

Davison, J.M., et al., 2007. Transactivation from Gal4-VP16 transgenic insertions for tissue-specific cell labeling and ablation in zebrafish. Dev. Biol. 304, 811–824.

Dias Moura Prazeres, P.H., et al., 2017. Pericytes are heterogeneous in their origin within the same tissue. Dev. Biol. 0–1. https://doi.org/10.1016/j.ydbio.2017.05.001.

Dobin, A., et al., 2013. STAR: ultrafast universal RNA-seq aligner. Bioinformatics 29, 15–21.

Du, K.L., et al., 2003. Myocardin is a critical serum response factor cofactor in the transcriptional program regulating smooth muscle cell differentiation. Mol. Cell. Biol. 23, 2425–2437.

Etchevers, H.C., Vincent, C., Le Douarin, N.M., Couly, G.F., 2001. The cephalic neural crest provides pericytes and smooth muscle cells to all blood vessels of the face and forebrain. Development 128, 1059–1068.

Filipek-Górniok, B., et al., 2015. The NDST gene family in Zebrafish: role of Ndst1b in pharyngeal arch formation. PLoS One 10, 1–19.

French, C.R., et al., 2014. Mutation of FOXC1 and PITX2 induces cerebral small-vessel disease. J. Clin. Investig. https://doi.org/10.1172/JCI75109.

Gays, D., et al., 2017. An exclusive cellular and molecular network governs intestinal smooth muscle cell differentiation in vertebrates. Development 144, 464–478.

Georgijevic, S., et al., 2007. Spatiotemporal expression of smooth muscle markers in developing zebrafish gut. Dev. Dynam. 236, 1623–1632.

Guo, D.C., et al., 2009. Mutations in smooth muscle alpha-actin (ACTA2) cause coronary artery disease, stroke, and moyamoya disease, along with thoracic aortic disease. Am. J. Hum. Genet. 84, 617–627.

Hartmann, D.A., et al., 2015. Pericyte structure and distribution in the cerebral cortex revealed by high-resolution imaging of transgenic mice. Neurophotonics 2, 041402.

Hayashi, H., Kume, T., 2008. Foxc transcription factors directly regulate DII4 and hey2 expression by interacting with the VEGF-notch signaling pathways in endothelial cells. PLoS One 3, 1–9.

Hayashi, H., Kume, T., 2008. Forkhead transcription factors regulate expression of the chemokine receptor CXCR4 in endothelial cells and CXCL12-induced cell migration. Biochem. Biophys. Res. Commun. 367, 584–589.

He, L., et al., 2016. Analysis of the brain mural cell transcriptome. Sci. Rep. 6, 35108.

Hellström, M., Kalén, M., Lindahl, P., Abramsson, A., Betsholtz, C., 1999. Role of PDGF-B and PDGFR-beta in recruitment of vascular smooth muscle cells and pericytes during embryonic blood vessel formation in the mouse. Development 126, 3047–3055.

Inman, K.E., Purcell, P., Kume, T., Trainor, P.A., 2013. Interaction between Foxc1 and Fgf8 during mammalian jaw patterning and in the pathogenesis of syngnathia. PLoS Genet. 9.

Isogai, S., Horiguchi, M., Weinstein, B.M., 2001. The vascular anatomy of the developing zebrafish: an atlas of embryonic and early larval development. Dev. Biol. 230, 278–301.

Joutel, A., et al., 1996. Notch3 mutations in CADASIL, a hereditary adult-onset condition causing stroke and dementia. Nature 383, 707–710.

Knight, R.D., 2003. Lockjaw encodes a zebrafish Tfap2a required for early neural crest development. Development 130, 5755–5768.

Kodo, K., et al., 2017. Regulation of Sema3c and the interaction between cardiac neural crest and second heart field during outflow tract development. Sci. Rep. 7, 6771.

Koo, H.Y., Kume, T., 2013. FoxC1-Dependent regulation of vascular endothelial growth factor signaling in corneal avascularity. Trends Cardiovasc. Med. 23, 4.

Kulkeaw, K., Sugiyama, D., 2012. Zebrafi Sh Erythropoiesis and the Utility of Fi Sh as Models of Anemia, vols. 1–11.

Kume, T., et al., 1998. The forkhead/winged helix gene Mf1 is disrupted in the pleiotropic mouse mutation congenital hydrocephalus. Cell 93, 985–996.

Kume, T., Jiang, H., Topczewska, J.M., Hogan, B.L.M., 2001. The murine winged helix transcription factors, Foxc1 and Foxc2, are both required for cardiovascular development and somitogenesis. Genes Dev. 15, 2470–2482.

Kwan, K.M., et al., 2007. The Tol2kit: a multisite gateway-based construction Kit for Tol2 transposon transgenesis constructs. Dev. Dynam. 236, 3088–3099.

Lamont, R.E., et al., 2010. Hedgehog signaling via angiopoietin1 is required for developmental vascular stability. Mech. Dev. 127, 159–168.

Lauter, G., Soll, I., Hauptmann, G., 2011. Two-color fluorescent in situ hybridization in the embryonic zebrafish brain using differential detection systems. BMC Dev. Biol. 11, 43.

Lee, M.Y., et al., 2015. Smooth muscle cell genome browser: enabling the identification of novel serum response factor target genes. PLoS One 10, 1–22.

Liao, Y., Smyth, G.K., Shi, W. FeatureCounts, 2014. An efficient general purpose program for assigning sequence reads to genomic features. Bioinformatics 30, 923–930.

Lindahl, P., Johansson, B.R., Levéen, P., Betsholtz, C., 1997. Pericyte loss and microaneurysm formation in PDGF-B-deficient mice. Science (80-.) 277, 242–245.

Liu, J., et al., 2007. A betaPix Pak2a signaling pathway regulates cerebral vascular stability in zebrafish. Proc. Natl. Acad. Sci. U. S. A. 104, 13990–13995.

Love, M.I., Huber, W., Anders, S., 2014. Moderated estimation of fold change and dispersion for RNA-seq data with DESeq2. Genome Biol. 15.

Majesky, M.W., 2007. Developmental basis of vascular smooth muscle diversity. Arterioscler. Thromb. Vasc. Biol. 27, 1248–1258.

Mears, A.J., et al., 1998. Mutations of the forkhead/winged-helix gene, FKHL7, in patients with Axenfeld-Rieger anomaly. Am. J. Hum. Genet. 63, 1316–1328.

Miesfeld, J.B., Link, B.A., 2014. Establishment of transgenic lines to monitor and manipulate Yap/Taz-Tead activity in zebrafish reveals both evolutionarily conserved and divergent functions of the Hippo pathway. Mech. Dev. 133, 177–188.

Mishra, S., Choe, Y., Pleasure, S.J., Siegenthaler, J.A., 2016. Cerebrovascular defects in Foxc1 mutants correlate with aberrant WNT and VEGF-A pathways downstream of retinoic acid from the meninges. Dev. Biol. 420, 148–165.

Mongera, A., et al., 2013. Genetic lineage labeling in zebrafish uncovers novel neural crest contributions to the head, including gill pillar cells. Development 140, 916–925.

Moura, D.A.P., Lemos, R.R., Oliveira, J.R.M., 2017. New data from pdfgbret/retMutant mice might lead to a paradoxical association between brain calcification, pericytes recruitment and BBB integrity. J. Mol. Neurosci. 63, 419–421.

Nishimura, D.Y., et al., 1998. The forkhead transcription factor gene FKHL7 is responsible for glaucoma phenotypes which map to 6p25. Nat. Genet. 19, 140–147.

Olson, L.E., Soriano, P., 2011. PDGFRβ signaling regulates mural cell plasticity and inhibits fat development. Dev. Cell 20, 815–826.

Omatsu, Y., Seike, M., Sugiyama, T., Kume, T., Nagasawa, T., 2014. Foxc1 is a critical regulator of haematopoietic stem/progenitor cell niche formation. Nature 508, 536–540.

Prasitsak, T., et al., 2015. Foxc1 is required for early stage telencephalic vascular development. Dev. Dynam. 244, 703–711.

Proulx, K., Lu, A., Sumanas, S., 2010. Cranial vasculature in zebrafish forms by angioblast cluster-derived angiogenesis. Dev. Biol. 348, 34–46.

Quillien, A., et al., 2017. Robust identification of developmentally active endothelial enhancers in zebrafish using FANS-assisted ATAC-seq. Cell Rep. 20, 709–720.

Santoro, M.M., Pesce, G., Stainier, D.Y., 2009. Characterization of vascular mural cells during zebrafish development. Mech. Dev. 126, 638–649.

Schilling, T.F., et al., 1996. Jaw and branchial arch mutants in zebrafish II: anterior arches and cartilage differentiation. Development 123, 345–356.

Schindelin, J., et al., 2012. Fiji: an open-source platform for biological-image analysis. Nat. Methods 9, 676–682.

Seiler, C., Abrams, J., Pack, M., 2010. Characterization of zebrafish intestinal smooth muscle development using a novel sm22α-b promoter. Dev. Dynam. 239, 2806–2812.

Seo, S., Kume, T., 2006. Forkhead transcription factors, Foxc1 and Foxc2, are required for the morphogenesis of the cardiac outflow tract. Dev. Biol. 296, 421–436.

Seo, S., et al., 2012. Forkhead box transcription factor FoxC1 preserves corneal transparency by regulating vascular growth. Proc. Natl. Acad. Sci. Unit. States Am. 109, 2015–2020.

Seo, S., et al., 2017. Foxc1 and foxc2 in the neural crest are required for ocular anterior segment development. Investig. Ophthalmol. Vis. Sci. 58, 1368–1377.

Siegenthaler, J.A., et al., 2013. Foxc1 is required by pericytes during fetal brain angiogenesis. Biol. Open 2, 647–659.

Skarie, J.M., Link, B.A., 2009. FoxC1 is essential for vascular basement membrane integrity and hyaloid vessel morphogenesis. Investig. Ophthalmol. Vis. Sci. 50, 5026–5034.

Souzeau, E., et al., 2017. Glaucoma spectrum and age-related prevalence of individuals with FOXC1 and PITX2 variants. Eur. J. Hum. Genet. 2559, 839–847.
Stratman, A.N., Malotte, K.M., Mahan, R.D., Davis, M.J., Davis, G.E., 2009. Pericyte recruitment during vasculogenic tube assembly stimulates endothelial basement membrane matrix formation. Blood 114, 5091–5101.
Stratman, A.N., et al., 2017. Interactions between mural cells and endothelial cells stabilize the developing zebrafish dorsal aorta. Development 144, 115–127.
Topczewska, J.M., et al., 2001. The winged helix transcription factor Foxc1a is essential for somitogenesis in zebrafish. Genes Dev. 15, 2483–2493.
Topczewska, J.M., Topczewski, J., Solnica-Krezel, L., Hogan, B.L.M., 2001. Sequence and expression of zebrafish foxc1a and foxc1b, encoding conserved forkhead/winged helix transcription factors. Mech. Dev. 100, 343–347.
Trost, A., et al., 2016. Brain and retinal pericytes: origin, function and role. Front. Cell. Neurosci. 10, 1–13.
Umali, J., Hawkey-noble, A., French, C.R., 2019. Loss of foxc1 in zebra fi sh reduces optic nerve size and cell number in the retinal ganglion cell layer ☆. Vis. Res. 156, 66–72.
Van Dijk, C.G.M., et al., 2015. The complex mural cell: pericyte function in health and disease. Int. J. Cardiol. 190, 75–89.
Vanlandewijck, M., et al., 2018. A molecular atlas of cell types and zonation in the brain vasculature. Nature 554, 475–480.
Veldman, M.B., Lin, S., 2012. Etsrp/Etv2 is directly regulated by Foxc1a/b in the zebrafish angioblast. Circ. Res. 110, 220–229.
Wang, Y., Pan, L., Moens, C.B., Appel, B., 2014. Notch3 establishes brain vascular integrity by regulating pericyte number. Development 141, 307–317.
Westerfield, M., 1995. In: The Zebrafish Book: A Guide for the Laboratory Use of Zebrafish (Danio Rerio). University of Oregon Press.
Whitesell, T.R., et al., 2014. An α-smooth muscle actin (acta2/αsma) zebrafish transgenic line marking vascular mural cells and visceral smooth muscle cells. PLoS One 9, 1–10.
Winkler, E.A., Bell, R.D., Zlokovic, B.V., 2010. Pericyte-specific expression of PDGF beta receptor in mouse models with normal and deficient PDGF beta receptor signaling. Mol. Neurodegener. 5, 32.
Winkler, E.A., et al., 2018. Reductions in brain pericytes are associated with arteriovenous malformation vascular instability. J. Neurosurg. 1–11. https://doi.org/10.3171/2017.6.JNS17860.
Xu, P., et al., 2018. Fox Proteins Are Modular Competency Factors for Facial Cartilage and Tooth Specification. https://doi.org/10.1242/dev.165498.
Yamagishi, H., et al., 2003. Tbx1 is regulated by tissue-specific forkhead proteins through a common Sonic hedgehog-responsive enhancer. Genes Dev. 17, 269–281.
Zarbalis, K., et al., 2007. Cortical dysplasia and skull defects in mice with a Foxc1 allele reveal the role of meningeal differentiation in regulating cortical development. Proc. Natl. Acad. Sci. U.S.A. 104, 14002–14007.